sections from sporadic CJD cases, neither of the chemicals labelled synaptic-type PrP deposition (data not shown). Non-specific labelling was barely observed after rinsing off the excess chemicals. As reported in previous studies (Mathis et al., 2002; Skovronsky et al., 2000), both chemicals stained senile plaques in Alzheimer's brain, and neither displayed signals in control brain sections without amyloid (data not shown). Similar results to those observed in the human TSE brain sections were obtained from post-mortem brains of Tg7 mice infected with the 263K strain; both chemicals stained the plaque-type PrP deposition in the cerebral white matter between the cortex and hippocampus (Fig. 2i–l). There was no PrP immunohistochemical signal or fluorescent signal in the brains of uninfected Tg7 mice (data not shown).

Since both BTA-1 and BSB have been reported to cross the blood–brain barrier, we performed in vivo experiments using Tg7 mice in a later stage of 263K scrapie infection. A bolus injection of BTA-1 labelled PrP plaques in the white matter between the cortex and hippocampus of the affected brains (Fig. 3a and b). Faint cerebrovascular labelling was occasionally observed at 4 h after the injection, but not at 18 h or later. PrP imaging of BSB in the brain in vivo was almost as effective as that of BTA-1 (Fig. 3c), but non-specific cerebrovascular labelling was more evident. Images of PrP deposition labelled by BSB were not clearly distinguishable in the cerebrovascular images until 24 h post-administration, but background staining was not seen thereafter. The stability of the signals of PrP deposition was examined at various time-points, and both chemicals remained stably visible at 42 h post-injection. In particular, the BSB labelling signals were relatively stable and visible even at 54 h post-injection. There was no significant

labelling after an injection of either chemical to uninfected transgenic mice upon examination after sacrifice 24 h later, or after an injection of vehicle alone to infected mice (data not shown). Similar results were obtained for Tga20 mice infected with the RML strain, although labelled PrP plaques were less frequently observed (data not shown).

Anti-prion activities in vitro and in vivo

The anti-prion activities of these chemicals were examined using three cell lines infected with different strains. Both BTA-1 and BSB inhibited PrP^{Sc} formation in ScN2a cells in a dose-dependent manner (Fig. 4a). The concentrations giving 50 % inhibition of PrP^{Sc} formation in ScN2a cells relative to the untreated control (IC_{50}) were 4 nM for BTA-1 and 1·4 μM for BSB. However, neither chemical was effective in the other cell lines (Fig. 4b and c). Treatment with vehicle (DMSO) alone showed no significant effects when compared with the untreated control. No apparent cell toxicity of the chemicals was observed up to 10 μM for BTA-1 and 100 μM for BSB. To examine the possibility of interference by the chemicals with immunodetection, BTA-1 or BSB at a concentration 10-fold higher than the IC_{50}s were added to lysates of untreated ScN2a cells for 1 h prior to proteinase K digestion. After these treatments, the PrP signals were not affected (data not shown).

Since BSB was potent without significant toxicity at a high concentration of 100 μM in the cell cultures and remained stably bound to PrP aggregates in the affected brains for more than 2 days in vivo, we examined whether BSB could be an effective treatment for TSE in two different experimental animal models. As shown in Fig. 5, treatment with BSB at 1 mg prolonged the incubation period of Tga20 mice
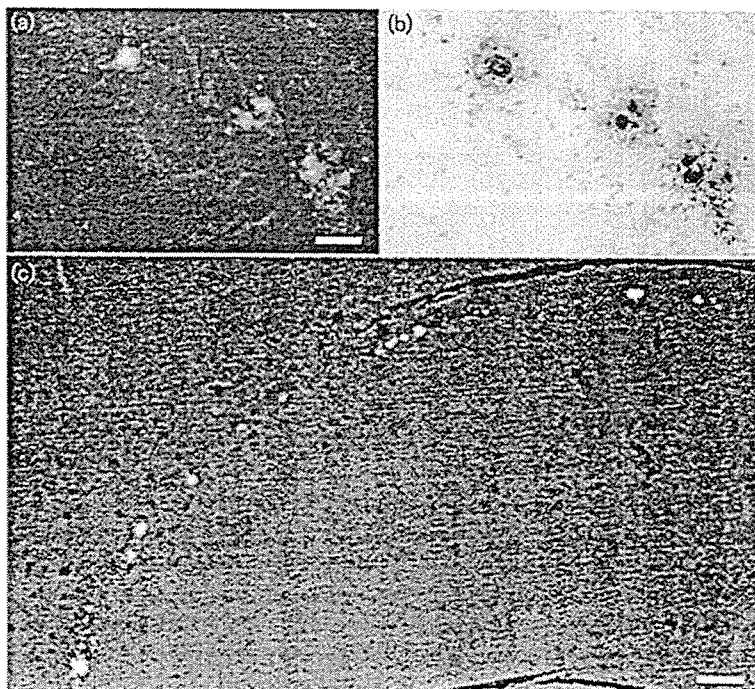

Fig. 3. In vivo imaging of PrP deposition in the brains of presymptomatic TSE-infected mice. An intravenous bolus injection of BTA-1 was given to Tg7 mice at 6 weeks post-infection, and they were sacrificed 24 h later. PrP plaques in the cerebral white matter between the cortex and hippocampus were detected under a fluorescent microscope (a), and then the brain section was immunostained for PrP (b). Similar results were observed with BSB (c, 24 h post-injection) and immunostaining for PrP (data not shown). Low magnification demonstrates PrP plaques in the cerebral white matter between the cortex and hippocampus were labelled with high specificity. All images are from coronal sections sited around one-third of the distance from the interaural line to the bregma line. Bars, 25 (a, b) and 100 (c) μm.
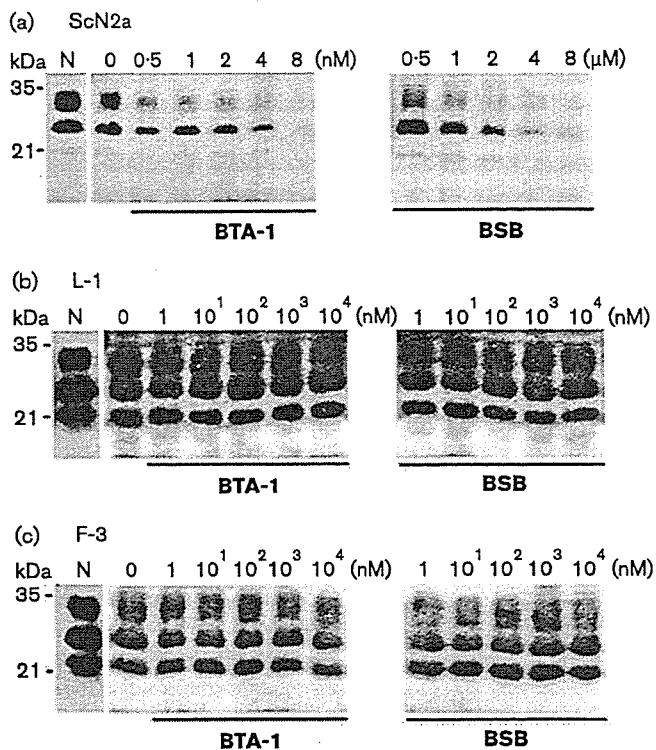
(a) ScN2a

(b) L-1

(c) F-3

Fig. 4. Inhibition of PrP^{Sc} formation in TSE-infected cells by BTA-1 or BSB. Various concentrations of each chemical were added to freshly passaged ScN2a cells in (a), L-1 cells in (b) and F-3 cells in (c), and the PrP^{Sc} levels were analysed by Western blotting. Lanes: N, untreated cells; 0, cells treated with vehicle (DMSO) alone. Bars on the left indicate molecular mass markers at 35 and 21 kDa.
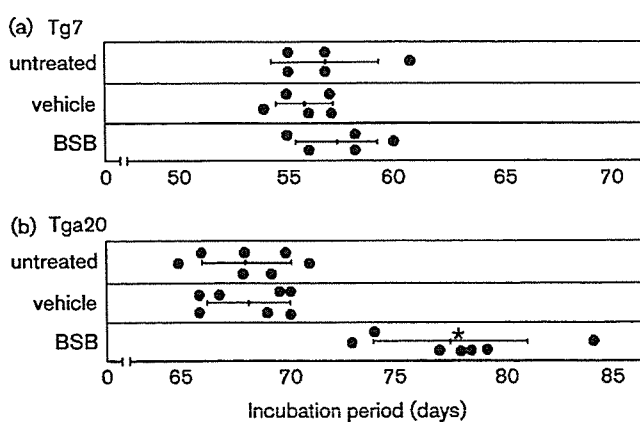

(a) Tg7

(b) Tga20

Incubation period (days)

Fig. 5. Effects of BSB treatment on TSE-infected mice. BSB was administered to Tg7 mice infected with the 263K strain (a) and Tga20 mice infected with the RML strain (b). The treatment protocol is described in the text. Each closed circle represents an individual animal. Bars represent the mean and standard deviation of the incubation periods of each group. *$P<0.0001$ versus the other groups.

infected with the RML strain by 13·6 % (77·6 ± 3·6 days in the BSB-treated group versus 68·3 ± 1·9 days in the vehicle control), whereas no significant prolongation was observed in the same treatment for Tg7 mice infected with the 263K strain (57·4 ± 1·9 days in the BSB-treated group versus 55·8 ± 1·3 days in the vehicle control). The dosage of BSB examined here corresponds to the concentration sufficient to detect PrP plaques *in vivo* as described above, and there were no apparent adverse effects of BSB. No significant differences in incubation times were observed between the untreated controls and the controls treated with vehicle (DMSO) alone (68·1 ± 2·1 days in the untreated control versus 68·3 ± 1·9 days in the vehicle control in Tga20 mice; 57·0 ± 2·4 days in the untreated control versus 55·8 ± 1·3 days in the vehicle control in Tg7 mice).

DISCUSSION

Both BTA-1 and BSB have been reported to be candidates for PET/SPECT tracers for the evaluation of Alzheimer's disease, and the results of this study have shown that they might also be useful for the evaluation of TSE with certain strains. However, the discrepancy in imaging between the plaque-type and the synaptic-type PrP deposition remains. A previous study demonstrated successful labelling of intracellular Aβ(1–42) accumulation in living cells by BSB (Skovronsky *et al.*, 2000), but the same chemical showed no labelling of PrP^{Sc} deposits in ScN2a cells (data not shown). These observations suggest that differences in the structures and/or the microenvironments of these PrP aggregates might account for the discrepancy. Further studies using more sensitive detection methods, such as the use of radiolabelling, might be helpful for evaluation.

Together with previous studies (Mathis *et al.*, 2002; Skovronsky *et al.*, 2000), the current study suggests that both BTA-1 and BSB label various amyloids including Aβ aggregates and PrP aggregates, and are not disease specific. However, these chemicals can be still useful to evaluate amyloid aggregates because anatomical distributions of pathological deposition are quite different between different diseases. For example, Aβ plaques are not, or seldom, observed in the cerebellum, while PrP amyloid plaques are predominantly observed there.

We also demonstrated therapeutic efficacies of these two chemicals. Congo red is well known to inhibit new formation of PrP^{Sc} in ScN2a cells and prolongs the incubation period of infected animals when administered prophylactically (Caughey *et al.*, 1993; Ingrosso *et al.*, 1995). However, Congo red cannot be used as a therapeutic drug because of its inability to cross the blood–brain barrier and its carcinogenicity due to its benzidine structure. BSB, a Congo red analogue, can enter the brain and lacks the benzidine structure. Here BSB showed a low toxicity and was as potent as Congo red in a cellular model, and furthermore, BSB-treatment prolonged the incubation period of the Tga20-RML infected mouse model despite being introduced at a late stage of TSE infection.

There was a discrepancy in the efficacy of BSB between Tg7 mice infected with the 263K strain and Tga20 mice infected with the RML strain. This discrepancy *in vivo* is consistent with that found *in vitro*, since BSB was only effective in ScN2a cells, which are infected with the RML strain. There is a possibility that the differences in susceptibility to these chemicals among the three cell lines might be caused by the differences in the expression levels of normal PrP, because the expression levels of normal PrP in L-1 cells or F-3 cells are five times higher than that of ScN2a cells. However, the data showed that the two chemicals had no effect in either L-1 cells or F-3 cells, even at doses five times greater than the IC_{50} in ScN2a cells. The findings suggest that the therapeutic efficacies of these chemicals are dependent on the TSE strain. In this study, we observed that the chemicals bound tightly to some kinds of PrP aggregates in the pathological sections of TSE, implying that a direct interaction with abnormal PrP molecules may play a role in the inhibition of PrP^{Sc} formation. However, the mechanism of the strain-specific efficacies of these chemicals remains to be elucidated.

Together with previous reports (Caughey *et al.*, 1993; Ingrosso *et al.*, 1995; Supattapone *et al.*, 2002), the current study demonstrated that chemicals with a high affinity for amyloid could be candidates for inhibiting PrP^{Sc} formation and increasing the life-span of TSE-infected animals. We tested this further by examining another chemical, 6-OH-BTA-1, which has recently been reported to facilitate PET studies of Alzheimer's disease (Engler *et al.*, 2002). We observed that this chemical inhibited PrP^{Sc} formation in ScN2a cells with an IC_{50} in the nanomolar order (data not shown), but *in vivo* studies remain to be performed.

In conclusion, BTA-1 and BSB, known as amyloid imaging probes, detected PrP deposition in the TSE brains both *in vitro* and *in vivo* and had anti-prion activities both *in vitro* and *in vivo*, although the efficacy depended upon the strain of TSE. These observations suggest that both could be lead chemicals not only for imaging probes, but also for therapeutic drugs for TSEs caused by certain strains.

ACKNOWLEDGEMENTS

REFERENCES

Bacskai, B. J., Klunk, W. E., Mathis, C. A. & Hyman, B. T. (2002). Imaging amyloid-β deposits *in vivo*. *J Cereb Blood Flow Metab* 22, 1035–1041.

Caughey, B. & Raymond, G. J. (1993). Sulfated polyanion inhibition of scrapie-associated PrP accumulation in cultured cells. *J Virol* 67, 643–650.

Caughey, B., Ernst, D. & Race, R. E. (1993). Congo red inhibition of scrapie agent replication. *J Virol* 67, 6270–6272.

Demaerel, P., Baert, A. L., Vanopdenbosch, L., Robberecht, W. & Dom, R. (1997). Diffusion-weighted magnetic resonance imaging in Creutzfeldt-Jakob disease. *Lancet* 349, 847–848.

Doh-ura, K., Mekada, E., Ogomori, K. & Iwaki, T. (2000). Enhanced CD9 expression in the mouse and human brains infected with transmissible spongiform encephalopathies. *J Neuropathol Exp Neurol* 59, 774–785.

Engler, H., Nordberg, A., Blomqvist, G. & 11 other authors (2002). First human study with a benzothiazole amyloid-imaging agent in Alzheimer's disease and control subjects. *Neurobiol Aging* 23, S429.

Fischer, M., Rulicke, T., Raeber, A., Sailer, A., Moser, M., Oesch, B., Brandner, S., Aguzzi, A. & Weissmann, C. (1996). Prion protein (PrP) with amino-proximal deletions restoring susceptibility of PrP knockout mice to scrapie. *EMBO J* 15, 1255–1264.

Hamad, A., Hamad, A., Sokrab, T. E., Momeni, S. & Brown, P. (2001). Iatrogenic Creutzfeldt-Jakob disease at the millennium. *Neurology* 56, 987.

Ingrosso, L., Ladogana, A. & Pocchiari, M. (1995). Congo red prolongs the incubation period in scrapie-infected hamsters. *J Virol* 69, 506–508.

Mathis, C. A., Bacskai, B. J., Kajdasz, S. T. & 8 other authors (2002). A lipophilic thioflavin-T derivative for positron emission tomography (PET) imaging of amyloid in brain. *Bioorg Med Chem Lett* 12, 295–298.

Murakami-Kubo, I., Doh-Ura, K., Ishikawa, K., Kawatake, S., Sasaki, K., Kira, J., Ohta, S. & Iwaki, T. (2004). Quinoline derivatives are therapeutic candidates for transmissible spongiform encephalopathies. *J Virol* 78, 1281–1288.

Murata, T., Shiga, Y., Higano, S., Takahashi, S. & Mugikura, S. (2002). Conspicuity and evolution of lesions in Creutzfeldt-Jakob disease at diffusion-weighted imaging. *Am J Neuroradiol* 23, 1164–1172.

Nishida, N., Harris, D. A., Vilette, D., Laude, H., Frobert, Y., Grassi, J., Casanova, D., Milhavet, O. & Lehmann, S. (2000). Successful transmission of three mouse-adapted scrapie strains to murine neuroblastoma cell lines overexpressing wild-type mouse prion protein. *J Virol* 74, 320–325.

Priola, S. A., Raines, A. & Caughey, W. S. (2000). Porphyrin and phthalocyanine antiscrapie compounds. *Science* 287, 1503–1506.

Prusiner, S. B. (1991). Molecular biology of prion diseases. *Science* 252, 1515–1522.

Race, R. E., Caughey, B., Graham, K., Ernst, D. & Chesebro, B. (1988). Analyses of frequency of infection, specific infectivity, and prion protein biosynthesis in scrapie-infected neuroblastoma cell clones. *J Virol* 62, 2845–2849.

Race, R. E., Priola, S. A., Bessen, R. A., Ernst, D., Dockter, J., Rall, G. F., Mucke, L., Chesebro, B. & Oldstone, M. B. (1995). Neuron-specific expression of a hamster prion protein minigene in transgenic mice induces susceptibility to hamster scrapie agent. *Neuron* 15, 1183–1191.

Skovronsky, D. M., Zhang, B., Kung, M. P., Kung, H. F., Trojanowski, J. Q. & Lee, V. M. (2000). *In vivo* detection of amyloid plaques in a mouse model of Alzheimer's disease. *Proc Natl Acad Sci U S A* 97, 7609–7614.

Supattapone, S., Nishina, K. & Rees, J. R. (2002). Pharmacological approaches to prion research. *Biochem Pharmacol* 63, 1383–1388.

Will, R. G., Ironside, J. W., Zeidler, M. & 7 other authors (1996). A new variant of Creutzfeldt-Jakob disease in the UK. *Lancet* 347, 921–925.

Yokoyama, T., Kimura, K. M., Ushiki, Y., Yamada, S., Morooka, A., Nakashiba, T., Sassa, T. & Itohara, S. (2001). *In vivo* conversion of cellular prion protein to pathogenic isoforms, as monitored by conformation-specific antibodies. *J Biol Chem* 276, 11265–11271.

A Pitfall in Diagnosis of Human Prion Diseases Using Detection of Protease-resistant Prion Protein in Urine

CONTAMINATION WITH BACTERIAL OUTER MEMBRANE PROTEINS*

Hisako Furukawa‡§, Katsumi Doh-ura¶, Ryo Okuwaki‖ Susumu Shirabe** Kazuo Yamamoto‖, Heiichiro Udono‡‡, Takashi Ito§§, Shigeru Katamine‖, and Masami Niwa‡

From the ‡Departments of Pharmacology 1, ‖Molecular Microbiology and Immunology, the **First Department of Internal Medicine, §§Department of Biochemistry, Nagasaki University Graduate School of Biomedical Sciences, 1-12-4 Sakamoto, Nagasaki 852-8523, Japan, the ¶Department of Prion Research, Tohoku University Graduate School of Medicine, 2-1 Seiryo-cho, Sendai 980-8575, Japan, and the ‡‡Laboratory for Immunochaperones, Research Center for Allergy and Immunology, RIKEN Yokohama Institute, Tsurumi, Yokohama 230-0045, Japan

Because a definite diagnosis of prion diseases relies on the detection of the abnormal isoform of prion protein (PrP^{Sc}), it has been urgently necessary to establish a non-invasive diagnostic test to detect PrP^{Sc} in human prion diseases. To evaluate diagnostic usefulness and reliability of the detection of protease-resistant prion protein in urine, we extensively analyzed proteinase K (PK)-resistant proteins in patients affected with prion diseases and control subjects by Western blot, a coupled liquid chromatography and mass spectrometry analysis, and N-terminal sequence analysis. The PK-resistant signal migrating around 32 kDa previously reported by Shaked et al. (Shaked, G. M., Shaked, Y., Kariv-Inbal, Z., Halimi, M., Avraham, I., and Gabizon, R. (2001) J. Biol. Chem. 276, 31479–31482) was not observed in this study. Instead, discrete protein bands with an apparent molecular mass of ~37 kDa were detected in the urine of many patients affected with prion diseases and two diseased controls. Although these proteins also gave strong signals in the Western blot using a variety of anti-PrP antibodies as a primary antibody, we found that the signals were still detectable by incubation of secondary antibodies alone, i.e. in the absence of the primary anti-PrP antibodies. Mass spectrometry and N-terminal protein sequencing analysis revealed that the majority of the PK-resistant 37-kDa proteins in the urine of patients were outer membrane proteins (OMPs) of the Enterobacterial species. OMPs isolated from these bacteria were resistant to PK and the PK-resistant OMPs from the Enterobacterial species migrated around 37 kDa on SDS-PAGE. Furthermore, nonspecific binding of OMPs to antibodies could be mistaken for PrP^{Sc}. These findings caution that bacterial contamination can affect the immunological detection of prion protein. Therefore, the presence of Enterobacterial species should be excluded in the immunological tests for PrP^{Sc} in clinical samples, in particular, urine.

Prion diseases are a group of neurodegenerative disorders pathologically characterized by accumulation of an abnormal isoform of prion protein (PrP^{Sc}) in the central nervous system. A definite diagnosis of prion diseases relies on the detection of PrP^{Sc} (1). Concerning the link between bovine spongiform encephalopathy and variant Creutzfeldt-Jakob disease (CJD),[1] the iatrogenic occurrence of prion diseases after dural transplantation, and the recent remarkable progress in therapeutic approaches have made it urgently necessary to establish a non-invasive in vivo test to enable a definite diagnosis of human prion diseases in the early or preclinical stage of the disease.

Diffusion-weighted magnetic resonance imaging of the brain is currently one of the most helpful techniques to detect abnormal high intensity lesions in the cerebral cortices and basal ganglia in the early stage of the disease (2). The detection of 14-3-3 proteins and measurement of phosphorylated tau protein in the cerebrospinal fluid has been found to be useful in supporting the clinical diagnosis of CJD (3,4). Although these tests are clinically useful, they are surrogate markers and therefore cannot provide direct evidence of the presence of PrP^{Sc}. Moreover, although a brain biopsy can reveal the deposition of PrP^{Sc} in the brain (5), it is highly invasive and is not suitable for preclinical screening or early diagnosis. Detection of PrP^{Sc} in body fluids such as blood and cerebrospinal fluid has been extensively investigated, but these tests still need a new technological device to increase the sensitivity (6).

As a potentially non-invasive diagnostic test, Shaked et al. (7) reported the presence of protease-resistant PrP in the urine (UPrP^{Sc}) of humans and animals affected with prion diseases. Their data suggests that UPrP^{Sc} will reflect the presence of PrP^{Sc} in the central nervous system and will also be a useful preclinical diagnostic test for prion diseases. In the present study, we have examined the urine protein of humans affected with prion diseases and controls using Western blot analysis to evaluate diagnostic usefulness and reliability of the UPrP^{Sc} assay in human prion diseases. A detailed analysis using coupled liquid chromatography and mass spectrometry (LC/MS) and N-terminal protein sequencing revealed that bacterial contamination might account for the misinterpretation in the interpretation of protease-resistant protein in urine.

[1] The abbreviations used are: CJD, Creutzfeldt-Jakob disease; PBS, phosphate-buffered saline; PK, proteinase K; OMP, outer membrane proteins.

Bacterial Contamination and Prion Protein in Urine

TABLE I

Protease-resistant protein in urine and characteristics of patients and controls

The abbreviations used are: GSS; Garstmann-Sträussler-Scheinker syndrome; HDS-R; revised Hasegawa Dementia Rating Scale; MMSE; Mini-Mental State Examination; and MELAS; mitochondrial myopathy, lactic acidosis, and stroke-like episodes.

Clinical diagnosis[a]	No. of cases	Mean age[b]	Mean clinical duration at examination	CSF 14–3–3 protein positive ratio	Brain DWI MRI[c] positive ratio	Protease-resistant protein in urine[d] positive ratio
		years	*months*		*%*	
Prion diseases						
Sporadic CJD	45	65.9 (42-83)	5.5 (1.5-18)	93.5 (29/31)	75.0 (15/20)	66.7 (30/45)
Dural graft-associated CJD	4	53.8 (15-69)	20.5 (6-48)	100 (3/3)	25.0 (1/4)	100 (4/4)
Familial CJD (E200K)	2	58.5 (53-64)	3.8 (3.5-4)	50 (1/2)	100 (2/2)	100 (2/2)
GSS (P102L)	3	57.3 (47-72)	45.3 (28-72)	NE[e]	NE	66.7 (2/3)
	54	58.9	9.58	91.7 (33/36)	69.2 (18/26)	70.4 (38/54)

				Mean scores		
				HDS-R	MMSE	
Diseased controls with dimentia						
Alzheimer's disease	19	74.2 (56-87)	NA[f]	13.5 (0-23)	18.8 (0-30)	0 (0/19)
Cerebrovascular dementia	1	76	NA	19	24	0 (0/1)
Diseased controls without dimentia						
Diabetes mellitus	7[g]	67.5 (53-75)	NA	NE	NE	14.3 (1/7)[h]
Cerebral infarction	6[g]	73.3 (62-77)	NA	NE	NE	16.7 (1/7)[h]
Multiple sclerosis	4	49.3 (24-62)	NA	NE	NE	25.0 (1/4)
Pneumonia	2	72.0 (70-74)	NA	NE	NE	0 (0/2)
Epilepsy	2	46.0 (20-72)	NA	NE	NE	0 (0/2)
Myasthenia gravis	1	35	NA	NE	NE	0 (0/1)
Encephalitis	1	57	NA	NE	NE	0 (0/1)
Chronic renal failure	1	79	NA	NE	NE	0 (0/1)
MELAS	1	21	NA	NE	NE	0 (0/1)
	23	27.5 (19-59)		NE	NE	0 (0/23)
Healthy controls		56.5				3 (2/66)

[a] Clinical diagnosis of prion diseases was performed in accordance with the criteria proposed by WHO.

[b] Mean age at onset in groups of prion diseases, at examination in controls.

[c] Abnormal high intensity signals in cerebral cortices or basal ganglia on diffusion-weighted (DWI) MRI of the brain.

[d] Determined by the presence of PK-resistant signal around 37 kDa.

[e] NE, not examined.

[f] NA, data not available.

[g] Two patients were included in both groups.

[h] Identical patient.

EXPERIMENTAL PROCEDURES

Analysis of Human Urine—Urine samples were collected from patients affected with prion diseases and control subjects under informed consent (Table I). A clinical diagnosis of prion disease was made by neurologists in order to follow the diagnostic criteria proposed by the World Health Organization (1). First morning urine samples were used whenever possible.

Protein was isolated from urine as previously described by Shaked *et al.* (7) with minor modifications. After dialysis and sedimentation by ultracentrifugation, the pellets obtained from 15 ml of urine were re-suspended in 30 μl of PBS (pH 7.4) containing 0.5% Nonidet P-40 and 0.5% sodium deoxycholate, instead of STE buffer containing 2% Sarkosyl, and digested with 40 μg/ml proteinase K (PK) (Roche Diagnostics) at 37 °C for 1 h. In several samples, urine protein was re-suspended in 2% Sarkosyl STE buffer prior to PK digestion as described by Shaked *et al.* (7). Western blot analysis was performed using monoclonal antibodies 3F4 at 1:10,000 (Signet Laboratories), 6H4 at 1:5,000 (Prionics, Switzerland), or 3O8 at 1:1,000 (Cayman Chemical) followed by incubation with donkey-derived anti-mouse IgG (AP192A, Chemicon), goat-derived anti-mouse IgG (H + L) (S372B, Promega), or the F(ab')₂ fragment of rabbit-derived anti-mouse IgG (710–4520, Rockland) and development in a chemiluminescent substrate (CDP Star or ECL-Plus, Amersham Biosciences). Some blots were labeled with PrP2B, rabbit-derived polyclonal antibody raised against PrP89-103, followed by incubation with donkey-derived anti-rabbit IgG (AP182A, Chemicon). In some blots, incubation with primary antibody was omitted for the experimental purpose.

Coupled Liquid Chromatography and Mass Spectrometry (LC/MS) Analysis of Protease-resistant Proteins—A PK-resistant signal of 37 kDa on a SDS-polyacrylamide gel was cut out and transferred to a clean, siliconized Eppendorf tube. In-gel digestion was performed as previously described (8). After an overnight incubation of gels with trypsin at 37 °C, the digested protein was extracted twice with 50% acetonitrile, 50% trifluoroacetic acid and concentrated by vacuum centrifugation. An LC/MS analysis was performed using the QSTAR XL system (Applied Biosystems) and MAGIC 2002 liquid chromatography

(Michrom BioResourse). The obtained protein masses were queried against entries for all species in the SwissProt data base using the Mascot Search program offered by Matrix Science.[2]

N-terminal Protein Sequencing—PK-resistant protein was obtained from the urine of patients sCJD 4, 5, and 7 and dural graft-associated CJD-1 as described above, or from urine of other patients as described by Shaked *et al.* (7). After separation of the protein samples by 12% mini SDS-PAGE gels (Bio-Rad), proteins were transferred onto Immobilon-P^SQ transfer membrane (Millipore). PK-resistant bands visualized by Coomassie Brilliant Blue staining were cut out and stored at 4 °C until the sequencing procedure. N-terminal protein sequencing by automated Edman degradation was performed using the Procise 491cLC protein sequencer (Applied Biosystems), as previously described (9). N-terminal sequencing proceeded for 13 to 23 cycles. The obtained amino acid sequences were queried against entries for all species in the SwissProt data base using the FASTA search program offered by GenomeNet.[3]

Assays of Protease Resistance of Outer Membrane Proteins (OMP)—OMPs were isolated from *Klebsiella pneumoniae* and *Salmonella typhimurium* as previously described (10) with minor modifications. In brief, cells harvested from overnight cultures in Super Broth medium were recovered by centrifugation. After washing with 10 mM Tris-HCl (pH 7.2), 5 mM MgCl₂, cells were broken by sonication. Unbroken cells were eliminated and cell envelopes were recovered at 100,000 × g for 1 h. After solubilization in 10 mM Tris-HCl (pH 7.2), 5 mM MgCl₂, 0.5% Nonidet P-40, 0.5% deoxycholate for 30 min at 25 °C, insoluble OMPs were recovered by ultracentrifugation at 100,000 × g for 1 h. OMPs were resuspended in 0.5% Nonidet P-40, 0.5% deoxycholate in PBS (pH 7.4), or 2% Sarkosyl STE buffer and digested with 40 μg/ml of PK at 37 °C for 1 h, under the same conditions as urine proteins. In parallel, 15 μg of ovalbumin was digested with PK as a control.

Binding of OMPs to F(ab')₂ Fragment of Immunoglobulin—Isolated OMPs were separated by 12% SDS-PAGE and transferred onto the

---

[2] Available at www.matrixscience.com.
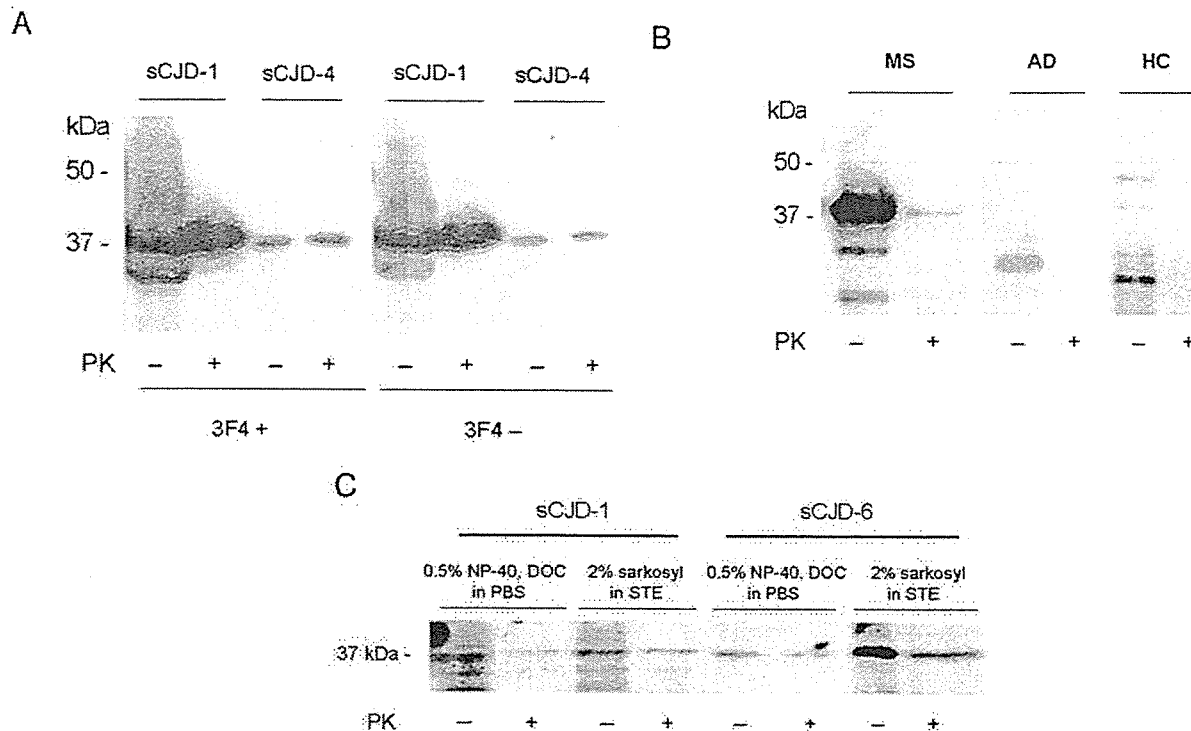
[3] fasta.genome.ad.jp.

FIG. 1. **Western blot analysis of urine proteins.** Protein obtained from 15 ml (*A* and *B*) or 7.5 ml (*C*) of urine was applied in each lane. *PK*, digestion with proteinase K. *A*, urine proteins were drawn from sCJD-1 and sCJD-4 patients. Patient ID number corresponds to that in Table III. Proteins were re-suspended in PBS (pH 7.4) containing 0.5% Nonidet P-40 and 0.5% deoxycholate (*DOC*). The blot was probed with 3F4 monoclonal antibody followed by incubation with secondary antibody AP192A (*left panel*) or incubated with secondary antibody omitting the probing with 3F4 (*right panel*). *B*, urine proteins were obtained from patients with multiple sclerosis (*MS*) bearing a urethral catheter, with Alzheimer's disease (*AD*), and from a healthy control subject (*HC*). Proteins were re-suspended in PBS (pH 7.4) containing 0.5% Nonidet P-40 and 0.5% deoxycholate. A PK-resistant signal was detected in one patient affected with MS. The membranes were probed with 3F4 monoclonal antibody followed by incubation with AP192A. *C*, urine proteins were drawn from sCJD-1 and sCJD-6 patients, and re-suspended in PBS (pH 7.4) containing 0.5% Nonidet P-40 and 0.5% deoxycholate or in STE buffer containing 2% Sarkosyl as described by Shaked *et al.* (7). The blot was incubated with a rabbit-derived F(ab')$_2$ fragment of anti-mouse IgG.

polyvinylidene difluoride membrane. To determine whether OMPs bind to antibodies via the Fc region of immunoglobulin, the membrane was incubated with the F(ab')$_2$ fragment of anti-mouse IgG conjugated with alkaline phosphatase (710–4520, Rockland) after blocking with 5% nonfat milk. The membrane was then developed in a chemiluminescent substrate (CDP Star, Amersham Biosciences).

RESULTS

PK-resistant Protein in the Urine of Humans Affected with Prion Diseases Directly Reacted with Secondary Antibodies— The results of urine protein examination and patient and control characteristics are summarized in Table I. We examined the PK sensitivity of urine proteins of patients affected with prion diseases (*n* = 54), healthy controls (*n* = 23), and disease control patients with (*n* = 20) and without dementia (*n* = 23). Clinical durations between disease onset and urine collection were 1.5 to 72 months in prion diseases. 14-3-3 protein in cerebrospinal fluid was frequently positive in sporadic CJD (93.5%, 29/31) and dural graft-associated CJD (100%, 3/3). Abnormal high intensity signals in the cerebral cortices or basal ganglia were observed in the majority of patients with sporadic CJD (75.0%, 15/20). Most patients carried methionine homozygosity at codon 129 in the prion protein gene (PRNP), except for one case that was affected with Gerstmann-Sträussler-Scheinker syndrome. No patients carried lysine polymorphisms at codon 219 in the PRNP.

Three kinds of signals migrating around 37, 28, and 22 kDa were observed after PK treatment of the urine. PK-resistant signals of 37 kDa were prominent and observed in all positive cases, whereas the other two signals were usually faint and not always observed in all the positive cases. The signals of 28 kDa were also observed in controls after digestion with PK, suggest-

ing that it represented a nonspecific signal because of PK itself. PK-resistant signals around 32 kDa, detected by Shaked *et al.* (7) in CJD patients, were not observed in the present study. Therefore, we decided to utilize the 37-kDa signal as a PK-resistant protein in urine in this study. PK-resistant protein signals of 37 kDa were detectable in 70.4% (38/54) of the patients affected with prion diseases, whereas 3% (2/66) of the control subjects were positive for PK-resistant signals. The PK-resistant signal was not detectable in healthy controls or diseased controls with dementia (Table I and Fig. 1*B*).

Although PK-sensitive and -resistant signals were detectable by labeling with 3F4 (Fig. 1*A*, *left panel*), 6H4, 3O8, or PrP2B (data not shown), these signals were also detectable with anti-mouse IgG antibody alone, omitting the incubation with 3F4 (Fig. 1*A*, *right panel*). This phenomenon was observed in all cases (11 cases; sporadic CJD, one case; dura-associated CJD) tested and reproducible using three kinds of anti-mouse IgG antibodies (AP192A, Chemicon; S372B, Promega; and 710–4520, Rockland) and an anti-rabbit IgG antibody (AP182A, Chemicon) (data not shown).

To examine the possible influence of assay conditions on the detection of PK-sensitive or -resistant signals, urine proteins were re-suspended prior to PK digestion in 2% Sarkosyl STE buffer as described previously by Shaked *et al.* (7) or in 0.5% Nonidet P-40, 0.5% deoxycholate, PBS buffer. As shown in Fig. 1*C*, 37-kDa signals were similarly detectable in both assay conditions, indicating that the difference of the assay conditions did not influence the detection of these signals.

Contamination of Urine with Bacterial Outer Membrane Proteins— To characterize the PK-resistant protein of 37 kDa on Western blot analysis, the bands from the urine of three pa-

TABLE II
List of proteins detected by LC/MS analysis
Protein masses were queried against entries for all species in the SwissProt database. Patient's ID correspond to that in Table III.

Patient ID	Significant hits		Peptides matched
	Protein identification	Species	
sCJD-1[a]	Outer membrane protein C precursor	*K. pneumoniae*	11
	Outer membrane protein C, chain A	*K. pneumoniae*	8
	Outer membrane protein C precursor	*S. typhimurium*	3
sCJD-2	Outer membrane protein C precursor	*E. coli*	13
	Outer membrane protein C precursor	*E. coli* O157:H7	13
	Outer membrane protein C precursor	*S. typhimurium*	4
	Translation initiation factor IF-2	*Geobacillus stearothermophilus*	3
	Outer membrane protein S2 precursor	*S. typhimurium*	2
	Outer membrane protein F precursor	*S. typhimurium*	2
sCJD-3	Outer membrane protein C precursor	*E. coli* O157:H7	16
	Outer membrane protein C precursor	*E. coli* O6	11
	Outer membrane protein C precursor	*S. typhimurium*	5
	Outer membrane protein C precursor	*K. pneumoniae*	4
	Outer membrane protein (fragment)	*Sodalis glossinidius*	2
	Outer membrane protein S1 precursor	*S. typhimurium*	2
	Outer membrane protein S2 precursor	*S. typhimurium*	2
	Outer membrane protein F precursor	*S. typhimurium*	2
	Glial fibrillary acidic protein homolog	*Carassius auratus*	2
	Elongation factor P-like protein	*S. typhimurium*	1

[a] sCJD, sporadic CJD.

tients were purified from the SDS-polyacrylamide gel and prepared for LC/MS as previously described (8). One of these patients was diagnosed as probable sporadic CJD and the others were pathologically definite sporadic CJD. Protein mass analysis using LC/MS demonstrated that the major component of the PK-resistant signal was the OMPs of bacteria such as *Escherichia coli*, *K. pneumoniae*, and *S. typhimurium* (Table II). No molecules of human origin, including PrP and immunoglobulin, were detected with any significance. Fig. 2 demonstrated the results of LC/MS analysis of a patient (sCJD-2).

We performed an N-terminal sequencing analysis to confirm the results of the LC/MS more quantitatively. It revealed that prominent PK-resistant signals in the urine of these three patients and all other patients examined (10/10) consisted of a mature chain of OMPs (Table III). Neither PrPs nor immunoglobulins were detected.

As described above, two other minor signals migrating around 28 and 22 kDa were observed on SDS-PAGE after PK treatment in the urine of some patients and controls. The N-terminal protein sequence analysis revealed that the signal at 28 kDa corresponded to the fragment of PK used for the assay and another signal at 22 kDa corresponded to the fragment of OMPs.

OMPs Are Resistant to PK—To evaluate PK sensitivity, OMPs were isolated from overnight cultured *K. pneumoniae* or *S. typhimurium* in Super Broth medium. After digestion with PK, a considerable amount of OMPs remained undigested and migrated around 37 kDa on SDS-PAGE (Fig. 3A, *fourth* and *sixth lanes*), whereas ovalbumin was completely digested under the same conditions (Fig. 3A, *second lane*). The electrophoretic mobility of PK-resistant OMPs was similar to that of the PK-resistant urine protein isolated from a patient affected with sporadic CJD (Fig. 3A, *seventh lane*).

OMPs Reacted with the F(ab') Portion of Immunoglobulins—To evaluate if OMPs bind to the Fc region of immunoglobulins like protein A, a cell wall component of *Staphylococcus aureus*, one of the gels was blotted onto a polyvinylidene difluoride membrane to perform Western blot analysis. As shown in Fig. 3B, OMPs bound to the F(ab')₂ fragment of anti-mouse IgG, indicating that OMPs bind to immunoglobulins in a manner that is different from that of protein A with immunoglobulins. This observation as well as PK resistance of

OMPs was not influenced by the difference in assay conditions (Fig. 3C).

DISCUSSION

In the present study, we found that the PK-resistant protein was frequently detected in the urine of patients affected with prion diseases. However, the LC/MS and N-terminal protein sequencing analysis revealed that the majority of PK-resistant proteins in the urine of patients, which migrated around 37 kDa on SDS-PAGE and reacted non-specifically with several secondary antibodies, comprised OMPs of bacteria such as *E. coli*, *K. pneumoniae*, and *S. typhimurium*, the popular causative agents for urinary tract infections. This finding indicated that bacterial contamination of urine might cause false-positive results in the assay for detecting UPrP^{Sc}.

It is known that urinary tract infections associated with urethral catheterization is the most common nosocomial infection and is often asymptomatic. In this study, the majority of patients affected with prion diseases were already bearing catheters because of severe deterioration of intellectual and motor functions as they were suspected to be suffering from prion diseases. Furthermore, two of the diseased control patients with positive PK-resistant urine protein were also bearing persistent or intermittent urethral catheters. One patient suffered from neurogenic bladder because of multiple sclerosis and another was long bedridden because of cerebral infarction. The signal intensity decreased after PK digestion in a patient affected with multiple sclerosis (Fig. 1B), whereas it was not significant in patients affected with sporadic CJD (Fig. 1A). Differences in bacterial species or growth conditions in urine between the cases might cause such a variation in PK sensitivity of OMPs. On the other hand, all diseased controls affected with Alzheimer's disease or cerebrovascular dementia were outpatients; therefore, they were thought to be at lower risk of urinary tract infections. These circumstances strongly supported that possible bacterial contamination resulted in the detection of confusing PK-resistant protein in urine.

OMPs are 36- to 39-kDa membrane spanning proteins that form channels in the outer membranes of Gram-negative bacteria. The primary and secondary structures of OMPs are well conserved in *Enterobacterial* species containing 16-stranded antiparallel β barrels to form channels (11). Biochemically,
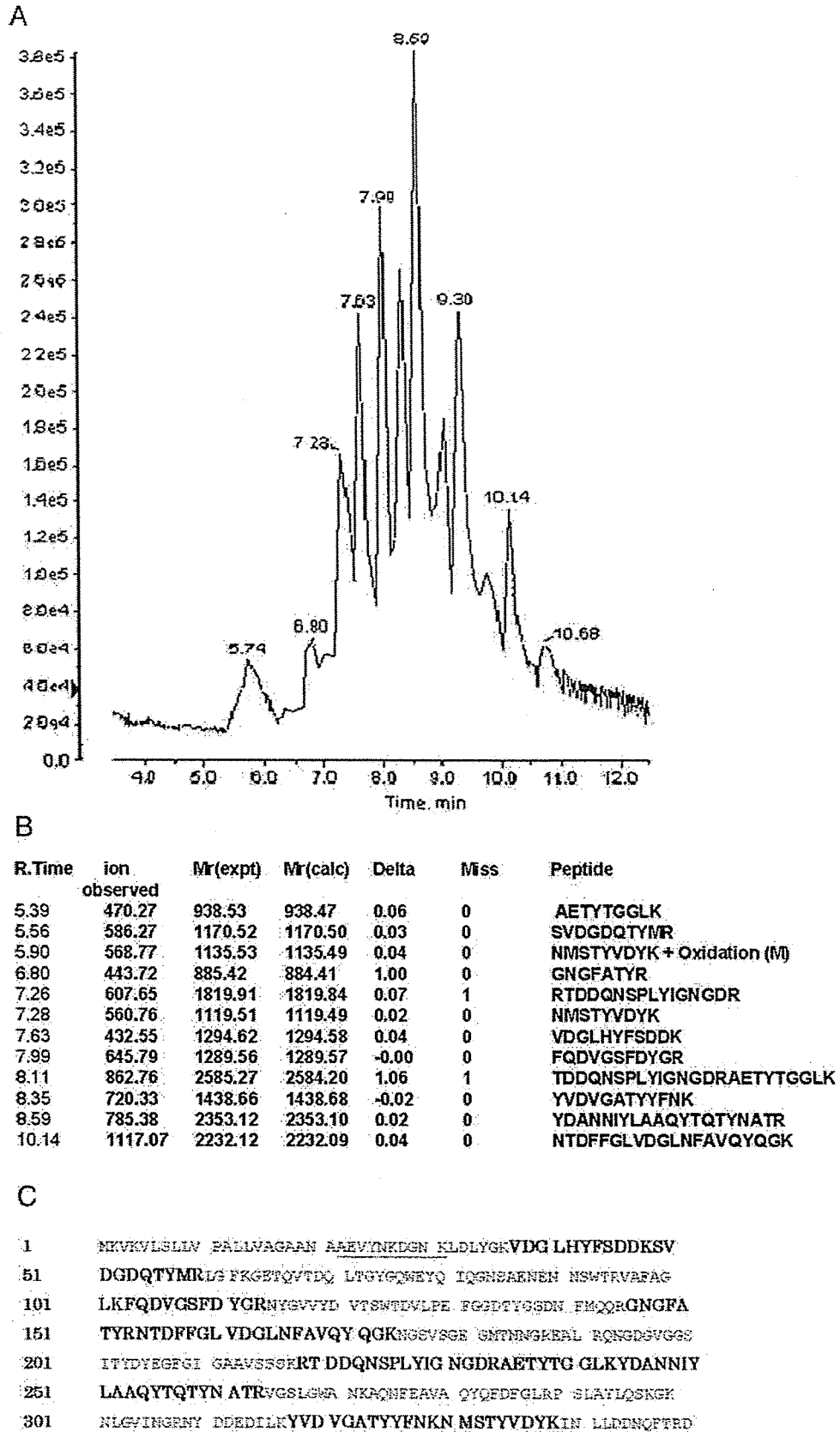
A

B

R.Time	ion observed	Mr(expt)	Mr(calc)	Delta	Miss	Peptide
5.39	470.27	938.53	938.47	0.06	0	AETYTGGLK
5.56	586.27	1170.52	1170.50	0.03	0	SVDGDQTYMR
5.90	568.77	1135.53	1135.49	0.04	0	NMSTYVDYK + Oxidation (M)
6.80	443.72	885.42	884.41	1.00	0	GNGFATYR
7.26	607.65	1819.91	1819.84	0.07	1	RTDDQNSPLYIGNGDR
7.28	560.76	1119.51	1119.49	0.02	0	NMSTYVDYK
7.63	432.55	1294.62	1294.58	0.04	0	VDGLHYFSDDK
7.99	645.79	1289.56	1289.57	-0.00	0	FQDVGSFDYGR
8.11	862.76	2585.27	2584.20	1.06	1	TDDQNSPLYIGNGDRAETYTGGLK
8.35	720.33	1438.66	1438.68	-0.02	0	YVDVGATYYFNK
8.59	785.38	2353.12	2353.10	0.02	0	YDANNIYLAAQYTQTYNATR
10.14	1117.07	2232.12	2232.09	0.04	0	NTDFFGLVDGLNFAVQYQGK

C

```
  1    MKVKVLSLLV PALLVAGAAN AAEVTNKDGN KLDLYGKVDG LHYFSDDKSV
 51    DGDQTYMRLG FKGETQVTDQ LTGYGQWEYQ IQGNSAENEN NSWTRVAFAG
101    LKFQDVGSFD YGRNYGVVYD VTSWTDVLPE FGGDTYGSDN FMQQRGNGFA
151    TYRNTDFFGL VDGLNFAVQY QGKNGSVSGE NTHNGREAL RQNGDGVGGS
201    ITYDYEGFGI GAAVSSSKRT DDQNSPLYIG NGDRAETYTG GLKYDANNIY
251    LAAQYTQTYN ATRVGSLGWA NKAQNFEAVA QYQFDFGLRP SLAYLQSKGK
301    NLGVINGRNY DDEDILKYVD VGATYYFNKN MSTYVDYKIN LLDDNQFTRD
```

FIG. 2. **LC/MS analysis of the PK-resistant protein in the urine.** Peptides from tryptic digestion of the PK-resistant protein in the urine of sCJD-3 were separated using MAGIC 2002 liquid chromatography and the elute were analyzed by MS. *A*, base peak mass chromatogram of the 37-kDa protein, each peak is labeled with the retention time. *B*, molecular mass and amino acid sequence of each peak originating from the 37-kDa protein. All the determined amino acid sequences were identical to that of OMP of *E. coli* (OmpC precursor) based on the results of the data base search. *R. Time*, retention time; *Mr(expt)*, molecular weight in the experiment; *Mr(calc)*, molecular weight in calculation. *C*, amino acid sequence of OmpC of *E. coli* was shown. *Bold style letters* indicate sequences covered by the results of the LC/MS analysis. The sequence identified by N-terminal sequencing analysis is shown with an *underline*.

Results of the N-terminal sequence of PK-resistant signal in patients' urine

Amino acid sequences were queried against entries for all species in the SwissProt database using the FASTA search programs offered by GenomeNet. PK-resistant protein bands with molecular mass about 37 kDa were subjected to the analysis.

Patient ID	N-terminal sequence	Protein identification and species
Sporadic CJD		
sCJD-1[a]	AEIYNKDGNK	OmpC, *K. pneumoniae*
sCJD-2[a]	AEVYNKDGNK	OmpC, *E. coli*
sCJD-3[a]	AEVYNKDGNK	OmpC, *E. coli*
sCJD-4	AEVYNKJDGNKLDLYGKVDGL	OmpC, *E. coli*
sCJD-5	AEIYNKDGNKLDLYG	OmpC, *K. pneumoniae*, or OmpF, *S. typhimurium*
sCJD-6[a]	AEVYNKDGNKLDLYG	OmpC, *E. coli*
sCJD-7	AEVLNKDONK	OmpC, *E. coli*
sCJD-8[a]	AEVYNKDGNKL	OmpC, *E. coli*
sCJD-9[a]	AEVYDKDGKNLDL	Omp *Sodalis glossinidius*
sCJD-10[a]	AEVYNKDGNKL	OmpC, *E. coli*
sCJD-11[a]	AEVYNKDGNKLDLYG	OmpC, *E. coli*
Dural graft-associated CJD		
1	AEVYNKDGNKLDLYG	OmpC, *E. coli*
2[a]	AEIYNKDGNKLDLYG	OmpC *K. pneumoniae*, or OmpF, *S. typhimurium*

[a] Urine samples were re-suspended in STE buffer containing 2% Sarkosyl as described by Shaked *et al.* (7) or otherwise in PBS containing 0.5% Nonidet P-40 and 0.5% deoxyehdate.
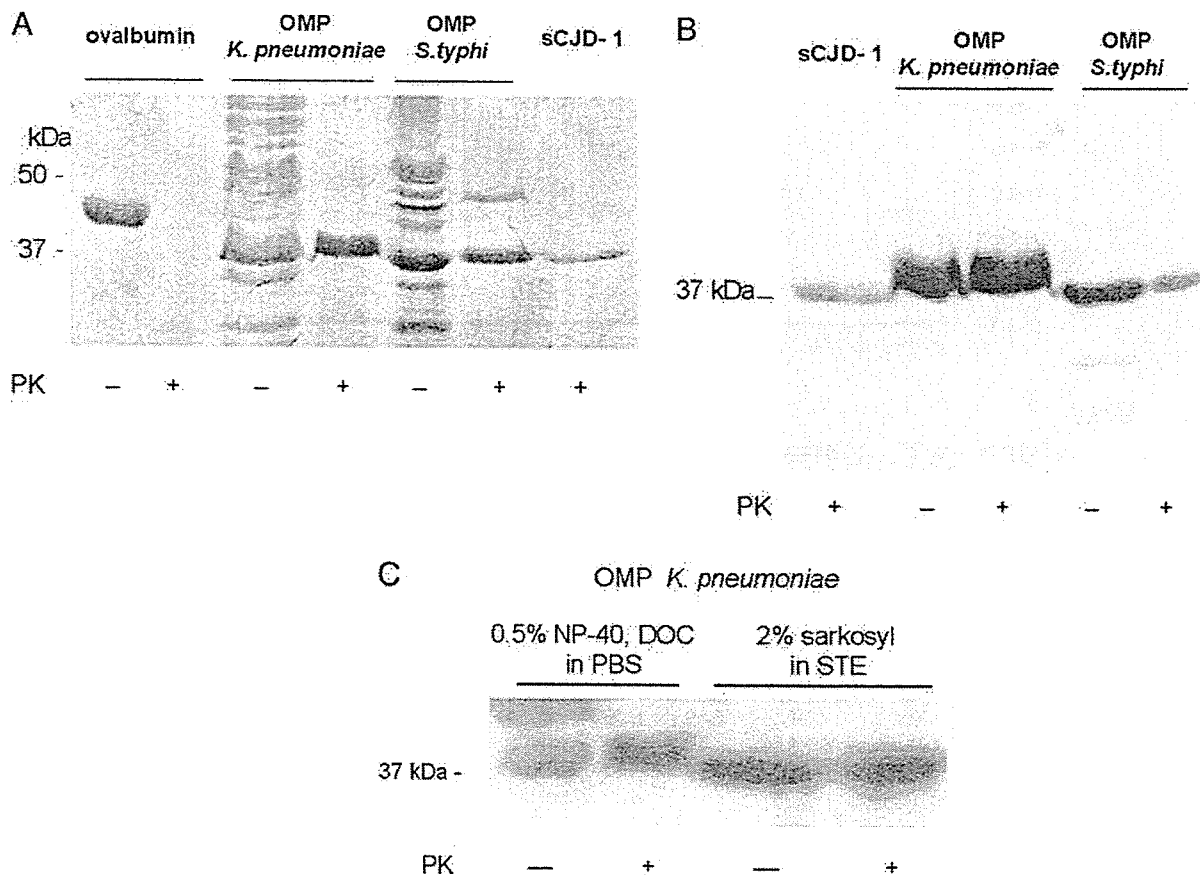
Fig. 3. **PK sensitivity and immunoreactivity of OMPs of *K. pneumoniae* and *S. typhimurium.** A*, OMPs isolated from *K. pneumoniae* and *S. typhimurium*, and protein isolated from 15 ml of urine of sCJD-1 patient were digested with PK. Proteins were re-suspended in PBS (pH 7.4) containing 0.5% Nonidet P-40 and 0.5% deoxycholate (*DOC*). An OMP homogenate containing 30 μg of protein was applied in each lane. Fifteen micrograms of ovalbumin was used as a control. After the electrophoretic separation, the polyacrylamide gel was stained with Coomassie Brilliant Blue. *B*, after separation by SDS-PAGE, the gel was blotted onto a polyvinylidene difluoride membrane. Rabbit-derived F(ab')₂ fragment of anti-mouse IgG was used as a probe. *C*, OMPs isolated from *K. pneumoniae* were re-suspended in PBS (pH 7.4) containing 0.5% Nonidet P-40 and 0.5% deoxycholate or in STE buffer containing 2% Sarkosyl and digested with PK. The blot was incubated with the rabbit-derived F(ab')₂ fragment of anti-mouse IgG.

OMPs are heat modifiable and resistant to trypsin (12). In this study, we have confirmed that OMPs of *K. pneumoniae* and *S. typhimurium* were also resistant to PK and the resulting molecules migrated around 37 kDa on SDS-PAGE.

OMPs act as a determinant of the permeability of antimicrobial agents and affect the interaction between bacteria and host defense mechanisms (13). Whereas it is known that the OMPs of *K. pneumoniae* bind to C1q (14), there are no previous reports that indicate the binding between OMPs and IgG. We found that OMPs bound non-specifically to IgG (several kinds of antibodies) during the procedure of Western blot analysis. Because protein A, a cell wall component of *S. aureus*, has been known to bind to the Fc region of IgG (15), we hypothesized that OMPs might also bind to IgG in the same manner. Contrary to our expectations, OMPs still reacted with the F(ab')₂ fragment of anti-mouse IgG, indicating that they bound to IgG

in a manner that is different from that of protein A with immunoglobulins. It might be suggested that accidentally acquired antibodies against bacterial OMPs in the serum of immunized animals might react with OMPs, resulting in protease-resistant signals. However, Western blot analysis using anti-mouse IgG produced by a phage-display method, for example, would be required to exclude this hypothesis.

Our findings were not consistent with those of a previous report by Shaked *et al.* (7). They showed that PK-resistant proteins in the urine of patients and animals affected with prion diseases were prion protein and termed them UPrP^{Sc}. The signal of UPrP^{Sc} showed a downward shift after PK digestion resulting in a 32-kDa fragment, whereas the majority of PK-resistant signals that we detected did not show a significant downward shift. Apart from the 37-kDa PK-resistant signal, a faint 22-kDa signal was observed in some patients and a 28-kDa signal was observed in both patients and controls. N-terminal sequencing revealed that these signals were fragments of OMPs and PK molecules, respectively. In this study, we did not observe any PK-resistant signals migrating around 32 kDa, which was detected by Shaked *et al.* (7) in the urine of patients. Therefore, the possibility that the PK-resistant molecule in this study might be a different molecule from UPrP^{Sc}, as demonstrated by Shaked *et al.* (7), was not excluded.

However, the high incidence of OMPs (37-kDa PK-resistant signals, non-specifically bind to immunoglobulins) in the urine of patients affected with prion diseases, irrespective of the assay conditions, indicated that bacterial contamination would always have to be considered in the application of a "UPrP^{Sc} assay" in the diagnosis of human prion diseases. Our findings suggest that PrP^{Sc} and PrP^{C} may not always exist or could exist at a very low level in urine, and bacterial contamination may often cause false detection of a PK-resistant isoform of prion protein in urine and a misinterpretation of results.

We have also analyzed the urine protein of mice experimentally infected with a prion agent. The PK-resistant signals of 25 kDa were found in the urine of affected mice, but these signals were also detectable using a secondary antibody alone, omitting the labeling by a primary antibody (data not shown). Furthermore, N-terminal sequencing analysis revealed that these PK-resistant signals in mice urine were OMPs of *Pseudomonas aeruginosa*.

In conclusion, the detection of UPrP^{Sc} is not useful or reliable for ante-mortem, definite diagnosis of human prion diseases in the present situation. Further improvement in sensitivity and specificity of this assay may make it a powerful diagnostic tool for prion diseases in the future.

REFERENCES

1. World Health Organization (2000) *WHO Infection Control Guidelines for Transmissible Spongiform Encephalopathies: Report of a WHO Consultation, Geneva, Switzerland, 23–26 March 1999*, Section 2.2, Communicable Disease Surveillance and Response (CSR), WHO
2. Demaerel, P., Baert, A. L., Vanopdenbosch, L., Robberecht, W., and Dom, R. (1997) *Lancet* **349,** 847–848
3. Hsich, G., Kenny, K., Gibbs, C. J., Lee, K. H., and Harrington, M. G. (1996) *N. Eng. J. Med.* **335,** 924–930
4. Riemenschneider, M., Wagenpfeil, S., Vanderstichele, H., Otto, M., Wiltfang, J., Kretzschmar, H., Vanmechelen, E., Forstl, H., and Kurz, A. (2003) *Mol. Psychiatry* **8,** 343–347
5. Castellani, R., Parchi, P., Stahl, J., Capellari, S., Cohen, M., and Gambetti, P. (1996) *Neurology* **46,** 1690–1693
6. Bieschke, J., Giese, A., Schulz-Schaeffer, W., Zerr, I., Poser, S., Eigen, M., and Kretzschmar, H. (2000) *Proc. Natl. Acad. Sci. U. S. A.* **97,** 5468–5473
7. Shaked, G. M., Shaked, Y., Kariv-Inbal, Z., Halimi, M., Avraham, I., and Gabizon, R. (2001) *J. Biol. Chem.* **276,** 31479–31482
8. Wilm, M., Shevchenko, A., Houthaeve, T., Breit, S., Schweigerer, L., Fotsis, T., and Mann, M. (1996) *Nature* **379,** 466–469
9. Morgenstern, J. P., Griffith, I. J., Brauer, A. W., Rogers, B. L., Bond, J. F., Chapman, M. D., and Kuo, M. C. (1991) *Proc. Natl. Acad. Sci. U. S. A.* **88,** 9690–9694
10. Hernández-Allés, S., Albertí, S., Álvarez, D., Doménech-Sánchez, A., Martínez-Martínez, L., Gil, J., Tomás, J. M., and Benedí, V. J. (1999) *Microbiology* **145,** 673–679
11. Weiss, M. S., Abele, U., Weckesser, J., Welte, W., Schiltz, E., and Schulz, G. E. (1991) *Science* **254,** 1627–1630
12. Albertí, S., Rodríquez-Quiòones, F., Schirmer, T., Rummel, G., Tomás, J. M., Rosenbusch, J. P., and Benedí, V. J. (1995) *Infect. Immun.* **63,** 903–910
13. Benz, R. (1994) in *Bacterial Cell Walls* (Ghuysen, J.-M., and Hackenbeck, R., eds) pp. 397–424, Elsevier, Amsterdam
14. Albertí, S., Marqués, G., Camprubí, S., Merino, S., Tomás, J. M., Vivanco, F., and Benedí, V. J. (1993) *Infect. Immun.* **61,** 852–860
15. Kessler, S. W. (1975) *J. Immunol.* **115,** 1617–1624

Quinoline Derivatives Are Therapeutic Candidates for Transmissible Spongiform Encephalopathies

Ikuko Murakami-Kubo,[1,2]* Katsumi Doh-ura,[1]* Kensuke Ishikawa,[1] Satoshi Kawatake,[1]†
Kensuke Sasaki,[1] Jun-ichi Kira,[2] Shigeru Ohta,[3] and Toru Iwaki[1]

*Departments of Neuropathology[1] and Neurology,[2] Graduate School of Medical Sciences, Kyushu University,
Fukuoka 812-8582, and Department of Graduate School of Biomedical Science, Hiroshima University,
Hiroshima 734-8551,[3] Japan*

We previously reported that quinacrine inhibited the formation of an abnormal prion protein (PrPres), a key molecule in the pathogenesis of transmissible spongiform encephalopathy, or prion disease, in scrapie-infected neuroblastoma cells. To elucidate the structural aspects of its inhibiting action, various chemicals with a quinoline ring were screened in the present study. Assays of the scrapie-infected neuroblastoma cells revealed that chemicals with a side chain containing a quinuclidine ring at the 4 position of a quinoline ring (represented by quinine) inhibited the PrPres formation at a 50% inhibitory dose ranging from 10^{-1} to 10^{1} μM. On the other hand, chemicals with a side chain at the 2 position of a quinoline ring (represented by 2,2′-biquinoline) more effectively inhibited the PrPres formation at a 50% inhibitory dose ranging from 10^{-3} to 10^{-1} μM. A metabolic labeling study revealed that the action of quinine or biquinoline was not due to any alteration in the biosynthesis or turnover of normal prion protein, whereas surface plasmon resonance analysis showed a strong binding affinity of biquinoline with a recombinant prion protein. In vivo studies revealed that 4-week intraventricular infusion of quinine or biquinoline was effective in prolonging the incubation period in experimental mouse models of intracerebral infection. The findings suggest that quinoline derivatives with a nitrogen-containing side chain have the potential of both inhibiting PrPres formation in vitro and prolonging the incubation period of infected animals. These chemicals are new candidates for therapeutic drugs for use in the treatment of transmissible spongiform encephalopathies.

Transmissible spongiform encephalopathies (TSEs), or prion diseases, are a group of fatal neurodegenerative disorders that include Creutzfeldt-Jakob disease and Gerstmann-Sträussler-Scheinker disease (GSS) in humans and scrapie, bovine spongiform encephalopathy, and chronic wasting disease in animals. These disorders are characterized by the accumulation of an abnormal isoform of prion protein (PrPres), which is high in beta-sheet content and resistant to digestion with proteases (15). Recent outbreaks in younger people of acquired forms of human TSEs, such as variant Creutzfeldt-Jakob disease (19) and iatrogenic Creutzfeldt-Jakob disease with cadaveric growth hormone or dura graft (4), are prompting the development of therapeutic interventions as well as early diagnostics.

One possible therapeutic strategy is to inhibit PrPres formation in the infected host. Doh-ura et al. first reported that cysteine protease inhibitors and lysomotropic agents inhibited PrPres formation in scrapie-infected neuroblastoma (ScNB) cells and that among them, quinacrine was one of the most

potent inhibitors (8). Another research group has also reported that quinacrine and its related tricyclic compounds are effective in inhibiting PrPres formation (11). Quinacrine is a synthesized chemical which has a quinoline ring in its structure. It is used as a substitute for quinine in the treatment of malaria. Accordingly, in this study we chose to focus on the quinoline derivatives to examine the structure-activity relationship involved in inhibiting PrPres formation as well as in prolonging the incubation time of infected animals.

MATERIALS AND METHODS

Chemicals and ScNB cells. Chemicals were purchased from Sigma, Maybridge (Cornwall, United Kingdom), Peakdale (Derbyshire, United Kingdom), Specs (Rijswijk, The Netherlands), and Bionet (Cornwall, United Kingdom) and were dissolved in 100% dimethyl sulfoxide (DMSO) or 96% ethanol just before use. ScNB cells (16) were grown in six-well culture plates in Opti-MEM (Invitrogen) supplemented with 10% fetal bovine serum. Chemicals at various concentrations were added to the medium when 1/20 of the confluent cells were passed. The final concentration of either DMSO or ethanol in the medium was less than 0.2%. The cultures were allowed to grow to confluence for 4 days.

Western blot analysis. PrPres was analyzed as described previously (5) with slight modification. Briefly, the cells in confluency were rinsed with phosphate-buffered saline (PBS) and lysed with lysis buffer (0.5% sodium deoxycholate, 0.5% Nonidet P-40, PBS). After low-speed centrifugation, the supernatant was treated with 10 μg of proteinase K/ml for 30 min at 37°C. Digestion was stopped with 0.5 mM phenylmethylsulfonyl fluoride, and the supernatant was centrifuged at 100,000 × g for 30 min at 4°C. Pellets were resuspended in 30 μl of the sample buffer by sonication. After being boiled, the sample was separated by electrophoresis on a Tris-glycine–sodium dodecyl sulfate–15% polyacrylamide gel electrophoresis (SDS-PAGE) and then electroblotted onto a polyvinylidene difluoride membrane (Millipore). The membrane was incubated with PrP-2B, an anti-PrP polyclonal antibody, against a mouse-hamster PrP fragment (amino acids 89 to 103) and then with an alkaline phosphatase-conjugated goat anti-

---

* Corresponding author. Mailing address for Ikuko Murakami-Kubo: Department of Neuropathology, Graduate School of Medical Sciences, Kyushu University, 3-1-1 Maidashi, Higashi-ku, Fukuoka 812-8582, Japan. Phone: 81-92-642-5537. Fax: 81-92-642-5540. E-mail: i-muraka@np.med.kyushu-u.ac.jp. Mailing address for Katsumi Doh-ura: Department of Prion Research, Tohoku University Graduate School of Medicine, 2-1 Seiryo-cho, Aoba-ku, Sendai 980-8575, Japan. Phone: 81-22-717-8232. Fax: 81-22-717-8148. E-mail: doh-ura@mail.tains.tohoku.ac.jp.

† Present address: Department of Prion Research, Tohoku University Graduate School of Medicine, Sendai 980-8575, Japan.

rabbit antibody (Promega). Signals were visualized with CDP-Star detection reagent (Amersham) and were densitometrically analyzed. Either the concentration of a chemical giving 50% inhibition of PrPres formation relative to the control 50% inhibitory concentration (IC_{50}) or the maximal concentration of a chemical that does not affect the rate of cell growth to confluence (TC) was estimated from more than three independent experiments.

Metabolic labeling study. Metabolic labeling of prion protein was performed as described previously (5). Briefly, subconfluent ScNB cells in 25-cm^2 flasks were rinsed three times with PBS and preincubated at 37°C in 1.5 ml of methionine-free minimal essential medium with 1% dialyzed fetal bovine serum and 1 μM quinine or 2,2'-biquinoline. After 60 min of preincubation, 125 μCi of ^{35}S-labeled methionine (Amersham) was added to each flask and incubated for 60 min. Then 10 ml of chase medium with 1 μM quinine or biquinoline was added, and the incubation was continued for 18 min, 2 h, or 8 h. Cells were rinsed three times with PBS and lysed with lysis buffer. After low-speed centrifugation, an aliquot of the supernatant was electrophoresed for total protein analysis; the remainder was used for immunoprecipitation of total prion protein. For the detection of cell surface phosphatidylinositol-anchored prion protein, cells were incubated for 30 min in the chase medium with 1 μM quinine or biquinoline after pulse labeling, rinsed three times with PBS, and then incubated with 1.33 U of phosphatidylinositol-specific phospholipase C (PIPLC)/ml in PBS at 37°C for 60 min. The soup was used for immunoprecipitation of cell-surface prion protein. Immunoprecipitation was performed with a PrP-2B antibody after whole proteins in the soup were precipitated with methanol and resuspended in detergent-lipid-protein complex solution.

Surface plasmon resonance sensorgram study. Interaction between prion protein and a chemical was analyzed using a BIAcore X systems. A recombinant murine prion protein fragment (amino acids 121 to 231) (PrP121-231) was immobilized on a sensor chip (CM5) according to the manufacturer's instructions. Each chemical was injected at a 100 μM concentration in running buffer (2.5% DMSO in PBS) for 1 min at a flow rate of 20 μl/min; then running buffer without a chemical was injected for 1 min at the same flow rate. Data were corrected by using a blank sensor chip as a control.

In vivo study. In vivo evaluation of the effectiveness of a chemical at prolonging the incubation times in infected animals was performed by using a mouse model of Tg7 (14, 17) or Tg20 (10), both of which have substantially shorter incubation periods than wild mice. Briefly, a 20-μl aliquot of 1% 263K pathogen homogenate for Tg7 mice, or the same amount of aliquot of 1% Rocky Mountain Laboratory (RML) pathogen homogenate or Fukuoka-1 pathogen homogenate for Tg20 mice, was inoculated into the right parietal portion of the brain. A 4-week continuous intraventricular infusion of vehicle alone (25% DMSO) or of a chemical dissolved in 25% DMSO was initiated at day 10 or 35 in Tg7 mice or at day 14 or 49 in Tg20 mice by using an Alzet osmotic pump equipped with a brain infusion kit (Durect, Cupertino, Calif.). An intraventricular infusion cannula from the brain infusion kit was fitted into the left frontal portion of the brain.

The infusion initiation date was selected at an early stage of the infection (day 10 or 14), or at a late stage (day 35 or 49), when abnormal PrP deposition in the brain definitely appeared in the 263K-infected Tg7 or RML-infected Tg20 mice. However, day 49 postinoculation in the Fukuoka-1-infected Tg20 mice was not exactly at a late stage of the infection, and no information on when abnormal PrP deposition appeared in this model was available.

In some experiments, intraperitoneal administration of a chemical was provided by a single injection once a day for 5 days per week from day 10 or day 35 postintracerebral inoculation until death. The incubation period during which the animals were observed every day lasted from the time of intracerebral infection until the time of death. Five male mice (each weighing about 30 g) per group were used in the experiments. Animal handling and killing were in accordance with national prescribed guidelines, with ethical approval for the study granted by the Animal Experiment Committee of Kyushu University.

Mice which died within a few days due to operational procedures were excepted from the statistical analysis after pathological confirmation. Doses of less than 8 nmol of quinine/day were examined, because toxicity shortened life span at doses beyond 8 nmol/day. Biquinoline was examined at doses of less than 16 nmol/day, which provided no toxicity yet solubility in 25% DMSO.

Immunohistochemistry. An indirect immunoperoxidase method was applied as described previously (9) with slight modification. Briefly, brains were obtained postmortem and fixed in 10% buffered formalin for several weeks. The tissue was immersed in 98% formic acid for 1 h to reduce infectivity and then embedded in paraffin. The samples were cut into 5-μm-thick sections, and then the sections were deparaffinized in xylene and hydrated using an ethanol gradient. The endogenous peroxidase activity was blocked with 0.3% H_2O_2 in absolute methanol for 30 min at r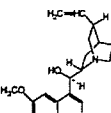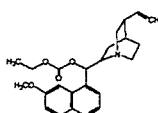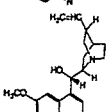oom temper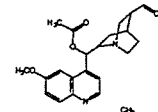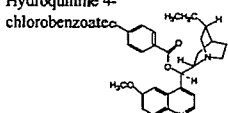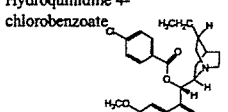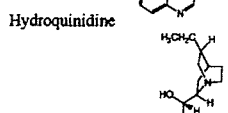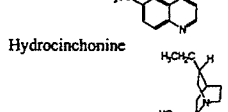ature. After being rinsed with tap water, the sections were treated with a hydrolytic autoclave (1 mM or 1.5 mM HCl, 121°C, 10 min) and washed in 50 mM Tris-HCl, pH 7.6, before being incubated with PrP-C polyclonal antibody (Immuno-Biological Laboratories, Gunma, Japan) (1:200) at 4°C overnight. The sections were then incubated with a horseradish peroxidase-conjugated secondary antibody (Vector Laboratories, Burlingame, Calif.) (1:200). The color reaction product was developed with 3,3'-diaminobenzidine tetrahydrochloride solution, and the sections were then counterstained with hematoxylin.
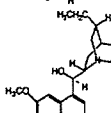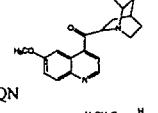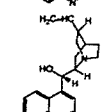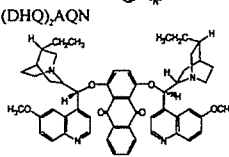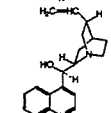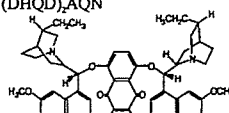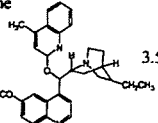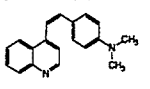
RESULTS

Screening of chemicals in vitro. Clinically available drugs with a quinoline ring and their related chemicals were first screened for the inhibition of PrPres formation in ScNB cells. The antimalarial drug quinine and its related chemicals (such as quinidine, hydroquinine, cinchonine, cinchonidine, and hydroquinidine 4-methyl-2-quinolyl ether) were found to be effective (Table 1, left column). The IC_{50} doses of these chemicals ranged from 3 to 18 μM, and the effective dose range between the IC_{50} and the TC was relatively narrow. Hydroquinidine 4-methyl-2-quinolyl ether, which has two quinoline rings, was slightly more effective than the chemicals with only one quinoline ring. Quinine-related chemicals with a carbonyl base located between a quinoline ring and a quinuclidine ring, such as MQAC (cinchonan-9-ol, 6'-methoxy-ethylcarbonate), MQAA (cinchonan-9-ol, 6'-methoxy-acetate), and MAM [(6-ethynyl-1-azabicyclo[2.2.2.]oct-2yl) (6-methoxy-4-quinolinyl) methanone], were more effective, and their IC_{50} dose ranges were 0.45 to 0.9 μM (Table 1, middle column). Chemicals with either the motif of quinine or that of quinidine on each lateral side of anthraquinone, $(DHQ)_2AQN$ (hydroquinine anthraquinone-1,4-diyl diether) and $(DHQD)_2AQN$ (hydroquinidine anthraquinone-1,4-diyl diether), were much more effective than those with only one motif, and their IC_{50} doses were 0.04 and 0.01 μM, respectively. A chemical with a 4-dimethylaminostyryl moiety was also very effective; and its IC_{50} was 0.012 μM. Except for this chemical, all of the effective chemicals shared a common structure composed of a quinoline ring plus a relative large side chain containing a quinuclidine ring at the 4 position of the quinoline ring. The chemicals listed in the right column of Table 1 also had this common structure, but they showed toxicity at a lower dose and were not effective within a nontoxic dose range.

Other quinoline chemicals unrelated to quinine were also screened. Chemicals with a side chain at the 2 position of a quinoline ring, such as 2,2'-biquinoline, inhibited PrPres formation at 0.003 μM, the minimum IC_{50} dose (Fig. 1A), and this effectiveness was reduced by the replacement of the quinoline ring by a pyridine ring or a naphthyridine ring (Table 2, left column). The addition of a carboxyl moiety to both the 4 position and the 4' position of the quinoline ring abolished the inhibiting activity of biquinoline (Table 2, right column, top). QCQH (8-hydroxy-8-quinolinylhydrazone-2-quinolinecarboxaldehyde) and PCQH (2-quinolinylhydrazone-2-pyridinecarboxaldehyde) were also very effective in inhibiting PrPres formation at an IC_{50} dose of 0.0075 and 0.004 μM, respectively. They shared a common structure with biquinoline respecting the arrangement of nitrogen atoms. DMEDAPQ (N,N-dimethyl-N'-[2-{4-pyridinyl}-4-quinolinyl]-1,2-ethanediamine) a chemical with a nitrogen-containing side chain at both the 2 position and the 4 position of a quinoline ring (thereby resem-

TABLE 1. Structure-activity relationship of quinine analogues on PrPres inhibition

	Effective							Ineffective			
Chemical	Structure	IC_{50} (μM)[a]	TC (μM)[b]	Chemical	Structure	IC_{50} (μM)[a]	TC (μM)[b]	Chemical	Structure	IC_{50} (μM)[a]	TC (μM)[b]
Quinine		6	50	MQAC		0.45	25	Hydroquinine 4-chlorobenzoate		-	5
Quinidine		3	>50	MQAA		0.5	>50	Hydroquinidine 4-chlorobenzoate		-	>5
Hydroquinine		12.5	50	MAM		0.9	>50	Hydroquinidine		-	2.5
Cinchonine		6	25	(DHQ)₂AQN		0.04	5	Hydrocinchonine		-	25
Cinchonidine		18	50	(DHQD)₂AQN		0.01	5				
Hydroquinidine 4-methyl-2-quinolyl ether		3.5	>5	4,(4-Dimethylaminostyryl) quinoline		0.012	10				

[a] IC_{50}, approximate concentration of a chemical giving 50% inhibition of PrPres formation relative to the control.
[b] TC, approximate maximal concentration of a chemical that does not affect the rate of cell growth to confluence.

bling quinine rather than biquinoline in terms of the arrangement of nitrogen atoms), was less effective than biquinoline, and its IC_{50} dose was 0.5 μM.

Chemicals containing a quinoline ring without a large side chain were also examined. They included quinoline hydrochloride, 8-hydroxyquinoline, 2,8-quinolinediol, 8-acetoxyquinoline, and CHIQ (5-chloro-7-iodo-8-quinolinol). All of them, with the exception of 2,8-quinolinediol, were ineffective at inhibiting PrPres within a nontoxic dose range (Table 2, right column). Quinolinediol showed an IC_{50} dose of 8 μM, which was much higher than those of other chemicals with a side chain at the 2 position of a quinoline ring (Table 2, left column, bottom).

Mechanism of inhibition of PrPres formation. Because quinine and biquinoline represented the effective chemicals found here, we focused on these chemicals and studied the mechanism behind their action. After ScNB cells had been treated with different concentrations of quinine or biquinoline for 4 days and then left without treatment for an additional 10 or 17 days, PrPres signals did not reappear even 17 days after discontinuation of the chemical treatment (Fig. 1B [for biquinoline] and data not shown [for quinine]). Thus, treatment with the chemicals permanently cured the cells of the accumulation of PrPres.

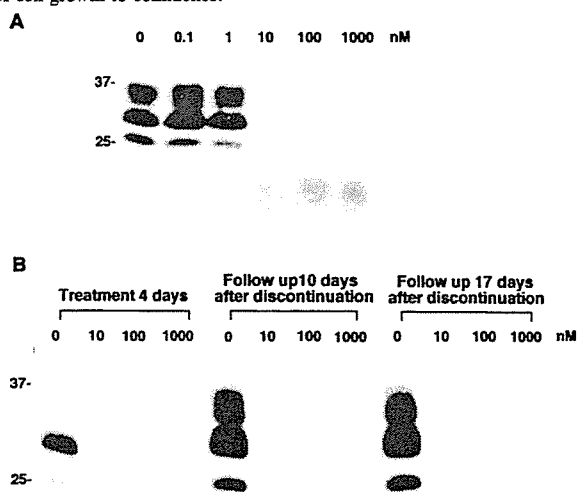Because phospholipase-sensitive cell surface PrP (PrPsen) is

FIG. 1. Inhibition of PrPres accumulation in ScNB cells grown with 2,2'-biquinoline (A) and lack of restoration of PrPres formation in ScNB cells treated once with biquinoline (B). (A) Biquinoline was added at designated concentrations to the medium when the cells were passed, and the culture was allowed to grow to confluence. Then, PrPres in the cells was analyzed by immunoblotting. (B) ScNB cells were treated with 10, 100, or 1,000 nM biquinoline for 4 days. The medium was replaced by fresh medium, and the cells were left without treatment for an additional 10 or 17 days. Then PrPres levels were assayed. Molecular size markers (in kilodaltons) are indicated.

TABLE 2. Structure-activity relationship of biquinoline analogues on PrPres inhibition

Effective				Ineffective			
Chemical	Structure	IC$_{50}$ (μM)^a	TC (μM)^b	Chemical	Structure	IC$_{50}$ (μM)^a	TC (μM)^b
2,2'-Biquinoline		0.003	>10	BQDA		-	>100
2-(2-Pyridinyl)quinoline		0.11	50	Quinoline hydrochloride		-	>25
2,2'-Bi(1,8-naphthyridine)		38	>100	8-Hydroxyquinoline		-	1
2-(2-Pyridinyl)-1,8-naphthyridine		12	200	8-Acetoxyquinoline		-	2.5
QCQH		0.0075	2.5	CHIQ		-	>5
PCQH		0.004	1				
DMEDAPQ		0.5	50				
2,8-Quinolinediol		8	>50				

^{a} IC$_{50}$, approximate concentration of a chemical giving 50% inhibition of PrPres formation relative to the control.
^{b} TC, approximate maximal concentration of a chemical that does not affect the rate of cell growth to confluence.

the precursor of PrPres, it is possible that the inhibition of PrPres accumulation by these chemicals was due to an indirect effect on PrPsen metabolism or turnover. However, biquinoline showed no effects on the metabolic labeling of cellular proteins or on the biosynthesis and turnover of PrPsen (Fig. 2A, B, and C).

Surface plasmon resonance analysis showed that the interaction of biquinoline with recombinant PrP121-231 occurred very slowly and failed to reach saturation even after 1 min. During the dissociation phase, furthermore, complete dissociation did not occur (Fig. 2D). On the other hand, the interaction of quinine or quinacrine occurred very quickly, reaching saturation within several seconds, and dissociation was completely over within seconds.

From observations of the structure of the effective chemicals, it was predicted that they might exert their inhibiting action through some mechanism which involved chelating metals. Thus, quinine and biquinoline were preincubated (before being added to the ScNB culture medium) with an equivalent dose of, a 10-times-higher dose of, or a 100-times-higher dose of various metal ions, including copper, zinc, manganese, iron, cobalt, and aluminum ions. The results showed no change in the inhibiting activities of the chemicals (data not shown).

In vivo study. To examine whether these chemicals could be effective in improving the prognosis in vivo, quinine or biquinoline was continuously administered intraventricularly in animal models which had been intracerebrally infected with three different TSE pathogen strains, comprising 263K scrapie agent, RML scrapie agent, and Fukuoka-1 GSS agent. Quinine administration from an early stage of infection prolonged the incubation period by 13.6% (days 47 to 53.4) at 0.64 nmol/day in 263K-infected mice (Fig. 3A), by 10.8% (days 68.6 to 76) at 1.6 nmol/day in RML-infected mice (Fig. 3B), and by 12.8% (days 104.2 to 117.5) at 0.64 nmol/day in Fukuoka-1-infected mice (Fig. 3C). The effect of quinine administration from a late stage of infection was clearly demonstrated in 263K-infected mice, resulting in 36% (days 47 to 63) prolongation of the incubation period at 1.6 nmol/day (Fig. 3A), with some of the RML-infected mice displaying a tendency to survive much longer than the control at 0.64 nmol/day (Fig. 3B). On the other hand, the effect of biquinoline administration was examined only in 263K-infected mice; it demonstrated 10.8% (days 49 to 54.3) prolongation of the incubation period in the group receiving 1.6 nmol/day at an early stage of infection, but no significant effects were observed in the groups which received it at a late stage (Fig. 3D). Intraperitoneal administration of biquinoline was also performed in 263K-infected mice, and this resulted in 7.7% (days 49 to 52.8) prolongation of the incubation period in the group receiving 0.39 mmol/day from an early stage of infection.

Postmortem histopathological examination of the brains treated with quinine or biquinoline was performed to see
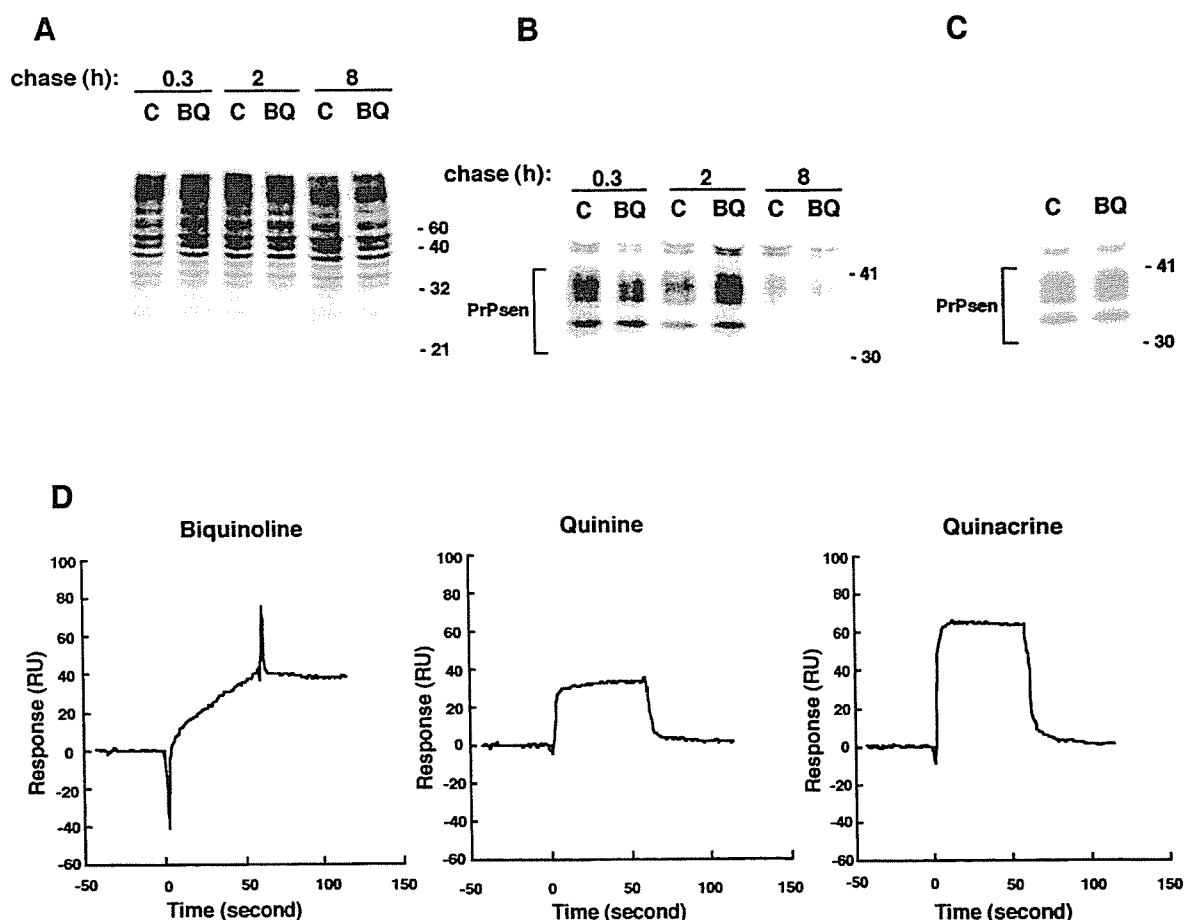
A

chase (h): __0.3__ __2__ __8__
             C BQ C BQ C BQ

- 60
- 40

- 32   PrPsen

- 21

B

chase (h): __0.3__ __2__ __8__
             C BQ C BQ C BQ

PrPsen [- 41

                                      - 30

C

                C   BQ

PrPsen [- 41

                        - 30

D

Biquinoline

Quinine

Quinacrine

FIG. 2. Lack of effect of the presence of biquinoline on the metabolic labeling of total protein (A), total PrPsen (B), and PIPLC-sensitive, cell surface PrPsen (C). (D) Direct interaction of biquinoline with recombinant PrP121-231 analyzed using a surface plasmon resonance sensorgram. (A) Control ScNB cells (lanes C) and biquinoline-treated cells (lanes BQ) were pulse labeled and then incubated in chase medium for the indicated chase time. The total lysate proteins were methanol precipitated from the detergent lysates of the cells and analyzed by SDS-PAGE. Equal flask equivalents were loaded onto all lanes in each panel. Molecular size markers (in kilodaltons) are indicated. (B) PrPsen was isolated from the total lysate proteins by immunoprecipitation and analyzed by SDS-PAGE. (C) PrPsen was immunoprecipitated from the cell soup treated with PIPLC. Biquinoline at 1 μM was included in all media, starting with the preincubation, except in the case of the control cells. (D) Interaction between a PrP121-231 fragment and a chemical was analyzed using a BIAcore system. A recombinant murine PrP121-231 fragment was immobilized on a CM5 sensor chip; biquinoline, quinine, or quinacrine (at 100 μM in buffer solution) was injected for 1 min at a flow rate of 20 μl/min for the association, and then the buffer solution without a chemical was injected at the same flow rate for the dissociation.

whether there was any modification in abnormal PrP deposition patterns following treatment. Those mice with prolonged incubation periods had a tendency to show less PrP deposition in the white matter between the cerebral cortex and the hippocampus of the brain hemisphere implanted with an intraventricular cannula, although they showed no apparent alteration in PrP deposition patterns in the bilateral thalamus or hypothalamus (Fig. 4).

DISCUSSION

In the studies reported here, we were able to identify quinoline derivatives that inhibited PrPres accumulation in ScNB cells. The commonly shared structure in these chemicals was a quinoline ring bound at its 2 or 4 position with a side chain containing a nitrogen atom, which was located at a particular distance from a nitrogen atom in the ring. Chemicals with a

side chain at the 2 position of a quinoline ring were more effective than those with a side chain at the 4 position. Replacement of a quinoline ring with a pyridine ring or a naphthyridine ring resulted in a weaker inhibiting activity, while modification of biquinoline by a moiety that caused less flexibility in the hinge portion between the quinoline rings completely suppressed the inhibiting activity. These findings suggest that a certain proper alignment of two nitrogens, one in a quinoline ring and the other in a side chain, might be important with regard to inhibiting activity.

As for the inhibiting mechanism of these chemicals, the representative chemicals, quinine and biquinoline, demonstrated no alteration either in the protein biosynthesis in general or in the metabolic labeling and turnover of PrPsen in particular. However, biquinoline showed a very strong binding affinity with recombinant PrP121-231 in the Biacore study. Thus, some of the chemicals, including biquinoline, may inhibit
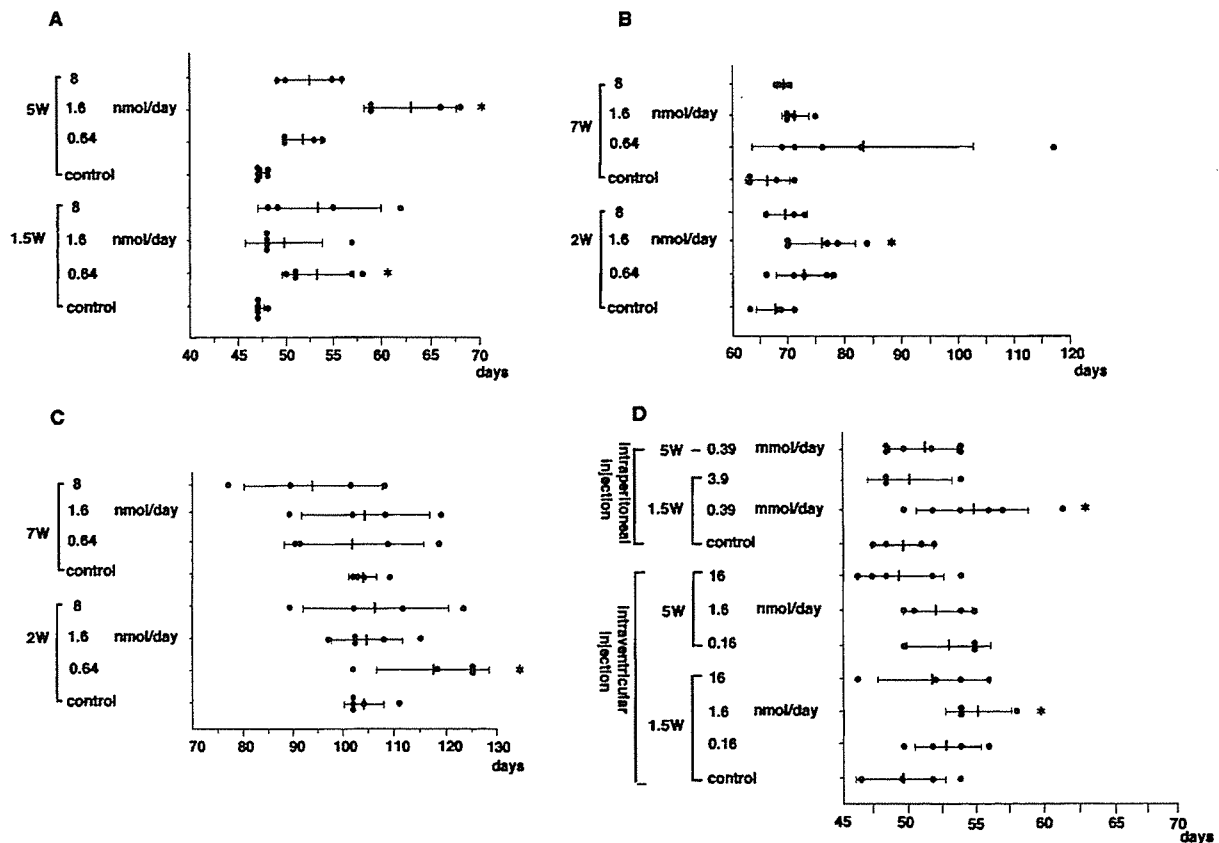
FIG. 3. Prolongation of incubation times in intracerebrally TSE-infected mice treated with quinine or biquinoline. (A) Tg7 mice infected with 263K agent strain and intraventricularly treated with quinine; (B) Tg20 mice infected with RML agent strain and intraventricularly treated with quinine; (C) Tg20 mice infected with Fukuoka-1 agent strain and intraventricularly treated with quinine; (D) Tg7 mice infected with 263K agent strain and intraperitoneally or intraventricularly treated with biquinoline. A 4-week continuous intraventricular infusion of a chemical was initiated by using an osmotic pump at day 10 (1.5W) or day 35 (5W) post-intracerebral inoculation in Tg7 mice or at day 14 (2W) or day 49 (7W) in Tg20 mice. For intraperitoneal treatment, injection of a chemical in Tg7 mice was performed intraperitoneally once a day for 5 days per week from day 10 (1.5W) or day 35 (5W) until the death of the mouse. Each closed circle represents the incubation time of an individual mouse. Each solid line and bar represent the average and standard deviation of the incubation times of each group. The star indicates groups with results with $P < 0.05$ compared to the results seen with the vehicle control. Each of the experiments was performed independently using different lots of the pathogen homogenate; thus, there was some variation in the data shown in panels A and D even for the same vehicle control.

the conversion of PrPsen to PrPres through direct interaction with PrPsen molecules. Since biquinoline (IC_{50} dose, 0.003 μM) was much more effective than quinine (3 μM) or quinacrine (at a concentration of 0.4 μM [8] or 0.3 μM [11]) in ScNB cells, the binding affinity of the PrP fragment (which was much stronger with biquinoline than with quinine or quinacrine) would appear to be clearly correlated with the inhibiting activity of PrPres formation in vitro. The potential binding site(s) of these chemicals in PrPsen molecules remains to be determined.

On the other hand, the involvement of chelating metal(s) in their inhibiting activity (as determined on the basis of the structure of the chemicals which were found to be effective in this study) was predicted. PrPsen is known to bind copper at its N-terminal octameric repeat region (3, 13, 18), and it is suggested that interaction between PrPres and copper stabilizes PrPres conformation (12). Manganese also binds PrP molecules instead of copper and increases proteinase K resistance and beta-sheet content (2). However, our observation suggests

that the chelating mechanism seems unlikely to be involved in the inhibiting action of the chemicals found here.

Among the chemicals tested here, CHIQ is an antibiotic (called clioquinol) and a Cu/Zn-selective chelator known to be effective in decreasing beta-amyloid deposits in Alzheimer's disease (6). However, in this study, CHIQ and its related compounds, quinoline hydrochloride, 8-hydroxyquinoline, and 8-acetoxyquinoline, did not inhibit PrPres formation in ScNB cells. These findings also suggest that chelating drugs which are effective in inhibiting beta-amyloid formation are not necessarily effective at inhibiting PrPres formation.

The in vivo study revealed that the chemicals with a quinoline ring were effective not only in inhibiting PrPres formation in vitro but also in prolonging incubation times of intracerebrally infected animals. The greatest effectiveness was obtained by intraventricular administration of quinine at 1.6 nmol/day, which prolonged the incubation time by 36% in 263K-infected mice (compared to the results seen with the control) when initiated at a late stage of infection. Quinine was also effective

A   B   C
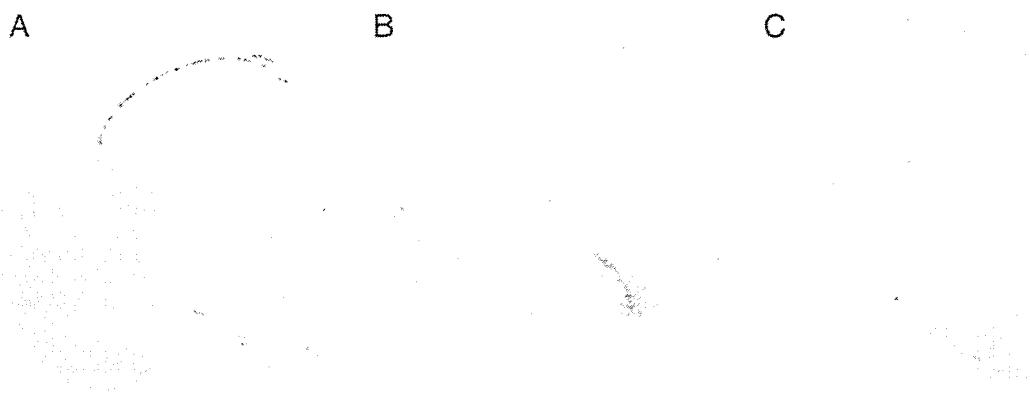
FIG. 4. Effects of intraventricular treatment with quinine or biquinoline on abnormal PrP deposition in the brain of intracerebrally 263K-infected Tg7 mice. The results for brain treated from day 10 postinfection for 4 weeks with vehicle (25% DMSO) alone (A), 0.64 nmol of quinine/day (B), or 1.6 nmol of biquinoline/day (C) are shown. Immunohistochemistry for abnormal PrP deposition was performed in the brains obtained postmortem from the longest-surviving members in each group, and representative examples of the brain hemisphere at the chemical injection side are shown.

in prolonging incubation times of the mice inoculated with different pathogen strains such as RML scrapie agent and Fukuoka-1 GSS agent. These findings indicate that application of quinine, an antimalarial drug, to humans infected with other TSE agents could be judicious.

Recently two research groups have reported that quinacrine is not effective in prolonging incubation times of intracerebrally infected TSE animals (1, 7). Our findings regarding quinine, which is a quinacrine-related chemical, appear to be inconsistent with their findings about quinacrine. However, differences in the structures of the chemicals and in the administration routes, doses, and durations as well as experimental models might have caused this gap but it remains to be elucidated.

Biquinoline was 1,000 times more effective than quinine in inhibiting PrPres formation in vitro with respect to the IC_{50} value, but when initiated from an early stage with intraventricular injections of 1.6 nmol/day or intraperitoneal injections of 0.39 mmol/day, its effectiveness in prolonging incubation times in vivo was clear, albeit marginal. The stability of chemicals and accessibility to targets in vivo might be different between these chemicals, and the reason for the gap between inhibiting activity in vitro and therapeutic activity in vivo remains to be found.

In investigations of the immunohistochemistry of the postmortem materials, abnormal PrP deposition in the white matter adjacent to the ventricle (where a chemical was injected continuously) was less evident in the mice treated with quinine or biquinoline from a early stage than in the control, although abnormal PrP deposition in the thalamus and hypothalamus was demonstrated in a fashion similar to that seen in the control. This would seem to imply that following treatment with a chemical, prolongation of incubation times in mice treated with the chemical might be associated with a reduction in abnormal PrP deposition in the brain.

In conclusion, we have demonstrated that quinoline derivatives with a relatively large side chain with a nitrogen are able to inhibit PrPres accumulation in ScNB cells and can prolong

the incubation periods of infected mice. The inhibition was not caused by interference in the biosynthesis or turnover of PrPsen or by the chelation of metals. Some of the chemicals, including quinine, are already in clinical use and are known to pass the blood-brain barrier. Thus, these drugs might be immediately available for clinical trials in investigations of the treatment of human TSEs.

REFERENCES

1. Barret, A., F. Tagliavini, G. Forloni, C. Bate, M. Salmona, L. Colombo, A. De Luigi, L. Limido, S. Suardi, G. Rossi, F. Auvre, K. T. Adjou, N. Sales, A. Williams, C. Lasmezas, and J. P. Deslys. 2003. Evaluation of quinacrine treatment for prion diseases. J. Virol. 77:8462–8469.
2. Brown, D. R., F. Hafiz, L. L. Glasssmith, B. S. Wong, I. M. Jones, C. Clive, and S. J. Haswell. 2000. Consequences of manganese replacement of copper for prion protein function and proteinase resistance. EMBO J. 19:1180–1186.
3. Brown, D. R., K. Qin, J. W. Herms, A. Madlung, J. Manson, R. Strome, P. E. Fraser, T. Kruck, A. von Bohlen, W. Schulz-Schaeffer, A. Giese, D. Westaway, and H. Kretzschmar. 1997. The cellular prion protein binds copper in vivo. Nature 390:684–687.
4. Brown, P., M. Preece, J. P. Brandel, T. Sato, L. McShane, I. Zerr, A. Fletcher, R. G. Will, M. Pocchiari, N. R. Cashman, J. H. d'Aignaux, L. Cervenakova, J. Fradkin, L. B. Schonberger, and S. J. Collins. 2000. Iatrogenic Creutzfeldt-Jakob disease at the millennium. Neurology 55:1075–1081.
5. Caughey, B., and G. J. Raymond. 1993. Sulfated polyanion inhibition of scrapie-associated PrP accumulation in cultured cells. J. Virol. 67:643–650.
6. Cherny, R. A., C. S. Atwood, M. E. Xilinas, D. N. Gray, W. D. Jones, C. A. McLean, K. J. Barnham, I. Volitakis, F. W. Fraser, Y. Kim, X. Huang, L. E. Goldstein, R. D. Moir, J. T. Lim, K. Beyreuther, H. Zheng, R. E. Tanzi, C. L. Masters, and A. I. Bush. 2001. Treatment with a copper-zinc chelator markedly and rapidly inhibits beta-amyloid accumulation in Alzheimer's disease transgenic mice. Neuron 30:665–676.
7. Collins, S. J., V. Lewis, M. Brazier, A. F. Hill, A. Fletcher, and C. L. Masters.

2002. Quinacrine does not prolong survival in a murine Creutzfeldt-Jakob disease model. Ann. Neurol. **52:**503–506.

8. **Doh-ura, K., T. Iwaki, and B. Caughey.** 2000. Lysosomotropic agents and cysteine protease inhibitors inhibit scrapie-associated prion protein accumulation. J. Virol. **74:**4894–4897.

9. **Doh-ura, K., E. Mekada, K. Ogomori, and T. Iwaki.** 2000. Enhanced CD9 expression in the mouse and human brains infected with transmissible spongiform encephalopathies. J. Neuropathol. Exp. Neurol. **59:**774–785.

10. **Fischer, M., T. Rulicke, A. Raeber, A. Sailer, M. Moser, B. Oesch, S. Brandner, A. Aguzzi, and C. Weissmann.** 1996. Prion protein (PrP) with amino-proximal deletions restoring susceptibility of PrP knockout mice to scrapie. EMBO J. **15:**1255–1264.

11. **Korth, C., B. C. May, F. E. Cohen, and S. B. Prusiner.** 2001. Acridine and phenothiazine derivatives as pharmacotherapeutics for prion disease. Proc. Natl. Acad. Sci. USA **98:**9836–9841.

12. **McKenzie, D., J. Bartz, J. Mirwald, D. Olander, R. Marsh, and J. Aiken.** 1998. Reversibility of scrapie inactivation is enhanced by copper. J. Biol. Chem. **273:**25545–25547.

13. **Miura, T., A. Hori-i, H. Mototani, and H. Takeuchi.** 1999. Raman spectroscopic study on the copper(II) binding mode of prion octapeptide and its pH dependence. Biochemistry **38:**11560–11569.

14. **Priola, S. A., A. Raines, and W. S. Caughey.** 2000. Porphyrin and phthalocyanine antiscrapie compounds. Science **287:**1503–1506.

15. **Prusiner, S. B.** 1991. Molecular biology of prion diseases. Science **252:**1515–1522.

16. **Race, R. E., B. Caughey, K. Graham, D. Ernst, and B. Chesebro.** 1988. Analyses of frequency of infection, specific infectivity, and prion protein biosynthesis in scrapie-infected neuroblastoma cell clones. J. Virol. **62:**2845–2849.

17. **Race, R. E., S. A. Priola, R. A. Bessen, D. Ernst, J. Dockter, G. F. Rall, L. Mucke, B. Chesebro, and M. B. Oldstone.** 1995. Neuron-specific expression of a hamster prion protein minigene in transgenic mice induces susceptibility to hamster scrapie agent. Neuron **15:**1183–1191.

18. **Viles, J. H., F. E. Cohen, S. B. Prusiner, D. B. Goodin, P. E. Wright, and H. J. Dyson.** 1999. Copper binding to the prion protein: structural implications of four identical cooperative binding sites. Proc. Natl. Acad. Sci. USA **96:**2042–2047.

19. **Will, R. G., J. W. Ironside, M. Zeidler, S. N. Cousens, K. Estibeiro, A. Alperovitch, S. Poser, M. Pocchiari, A. Hofman, and P. G. Smith.** 1996. A new variant of Creutzfeldt-Jakob disease in the UK. Lancet **347:**921–925.

Clinical features of Creutzfeldt–Jakob disease with V180I mutation

K. Jin, MD; Y. Shiga, MD, PhD; S. Shibuya, MD, PhD; K. Chida, MD, PhD; Y. Sato, MD, PhD;
H. Konno, MD, PhD; K. Doh-ura, MD, PhD; T. Kitamoto, MD, PhD; and Y. Itoyama, MD, PhD

Abstract—The authors describe the clinical features of Creutzfeldt–Jakob disease (CJD) with the causative point mutation at codon 180. The symptoms never started with visual or cerebellar involvement. The patients showed slower progression of the disease compared with sporadic CJD. They never showed periodic sharp and wave complexes in EEG. MRI demonstrated remarkable high-intensity areas with swelling in the cerebral cortex except for the medial occipital and cerebellar cortices. These characteristic MRI findings are an important clue for an accurate premortem diagnosis.

NEUROLOGY 2004;62:502–505

Approximately 10 to 15% of all Creutzfeldt–Jakob disease (CJD) cases are estimated to be familial.[1] Some of them are sporadic cases with no relevant family history because of incomplete genetic penetrance and the misdiagnosis of other affected family members. The clinical features depend on the genetic mutations. However, most patients demonstrate periodic sharp and wave complexes (PSWC) in EEG, an accepted diagnostic marker for CJD.

CJD with a causative point mutation of valine to isoleucine at codon 180 (V180I)[2-5] is a type of familial CJD with no relevant family history. In case reports, the clinical features of CJD with V180I (CJD180) were different from those of sporadic CJD (sCJD). Therefore, the premortem clinical diagnosis was difficult, and the cases had been misdiagnosed as neurodegenerative disorders with dementia. We herein report the clinical features and characteristic MRI findings of five original cases of CJD180 together with a review of four reported cases.

Patients and methods. *Patients.* Nine patients including our five original patients and four other previously reported pathologically verified patients[2-5] were studied retrospectively. The clinical features of these patients are shown in table 1. The previously reported case with a double mutation at codon 180 and codon 232 of the *PRNP* was excluded from this study because the codon 232 mutation might influence the clinical course.[6] All nine had neither family history of dementia nor obvious iatrogenic exposure. Their PRNP analyses at codon 129 revealed that four had methionine homozygosity (MM129) and five had methionine/valine heterozygosity (MV129), in which the V180I mutation and valine at codon 129 were on different alleles.

The common histopathologic findings in the five pathologically verified patients were evident spongiform changes in all layers of the cerebral cortex with less prominent neuronal loss and gliosis without Kuru plaque. Immunohistochemical analysis showed weak prion protein staining of the synaptic type in three of three patients examined.[2,4,5]

Methods. We compared the clinical features, laboratory findings, and MRI findings of the 9 patients with those of 123 patients (25 were pathologically verified) with genetically verified sCJD, which were reported to the Japanese CJD Surveillance Committee.[7] The *PRNP* analysis revealed that 116 of the 123 had MM129, 5 had MV129, and 2 had valine homozygosity at codon 129. We then compared the features between CJD180 and sCJD by dividing them into two groups: patients with MM129 and patients with MV129.

CSF was examined within 6 months from the onset for the differential diagnosis. The neuron-specific enolase (NSE) value in CSF was measured commercially using an ELISA method (SRL Laboratory, Tokyo, Japan), and a value of >35 ng/mL was considered positive.[8] The 14-3-3 protein immunoassay was performed by western blot using polyclonal antibody SC-629 (Santa Cruz Biotechnology, Santa Cruz, CA). EEG using the International 10–20 method was examined repeatedly during the disease course.

In the MRI study, T1-weighted (T1I), T2-weighted (T2I), fluid-attenuated inversion recovery (FLAIR), and diffusion-weighted (DWI) imaging was performed for Patients 1, 3, 4, and 5. T1I and T2I were performed for Patients 2, B,[3] and D.[5]

The Mann–Whitney *U* test was used for a comparison of the clinical findings and NSE values between CJD180 and sCJD. The Fisher exact probability test was used for a comparison of the positive rates of clinical symptoms, NSE, 14-3-3 protein, and PSWC.

Results. The results of the comparison between CJD180 and sCJD in each group, the MM129 group and MV129 group, are listed in table 2. The two groups had similar results, even though some were not statistically significant. CJD180 had an older onset age, longer duration from the onset to the appearance of myoclonic jerk that was less prominent compared with that of sCJD, longer duration from the onset to becoming akinetic and mute, lower value of NSE in CSF, and lower positive rate of NSE and 14-3-3 protein in CSF compared with those of sCJD. As cardinal symptoms, higher cortical dysfunctions such as aphasia and apraxia, which were not frequent symptoms in sCJD,

Table 1 *Patients' profiles in this study: five original and an additional four reported patients*

Clinical features	Original patients					Previously reported patients			
	Patient 1	Patient 2	Patient 3	Patient 4	Patient 5	Patient A[2]	Patient B[3]	Patient C[4]	Patient D[5]
Age at onset, y/sex	81/F	74/M	78/M	58/M	72/M	77/F	65/F	70/F	80/M
Duration until appearance of each clinical symptom, mo									
Myoclonic jerk	−*	5	8	10	4	6	14	9	+†
Visual or cerebellar symptom	−*	−‡	−‡	−§	−‡	−‡	−‡	−‡	−‡
Akinetic mutism	−*	12	18	−§	10	18	14	9	>18
Higher cortical dysfunction‖	−	−	+	+	+	−	+	+	+
Parkinsonism‖	−	−	+	−	−	+	−	−	−
NSE value in CSF, ng/mL	32.1	13.0	19.5	22.0	60.4	NE	NE	NE	29.9
14-3-3 protein in CSF	+	−	+	−	NE	NE	NE	NE	NE
Duration from onset to CSF study, mo	3	6	1	4	3	5	Uncertain	2	1
PSWC in EEG	−	−	−	−	−	−	−	−	−
Codon 129 in *PRNP*	M/V	M/M	M/V	M/V	M/M	M/V	M/M	M/M	M/V
PrP staining	NE	NE	NE	NE	NE	+	NE	+	±

Patient A was previously reported by Matsumura et al.[2] Patient B was previously reported by Ishida et al.[3] Patient C was previously reported by Kobayashi et al.[4] Patient D was previously reported by Iwasaki et al.[5]

* We could not detect referring symptoms during our observation period in Patient 1 (until 15 mo after the onset). † The duration until the appearance of myoclonic jerk in Patient D is uncertain. ‡ We or the authors could not detect visual or cerebellar symptoms during the observation period. The patients' severe dementia or consciousness disturbance prevented us from making a close neurologic examination in the advanced stage.
§ We could not detect the referring symptoms during our observation period in Patient 4 (until 16 mo after the onset).
‖ The presence or lack of presence as initial symptoms.

NSE = neuron-specific enolase; NE = not examined; PSWC = periodic sharp and wave complexes; *PRNP* = prion protein gene; M/V = methionine/valine heterozygosity at codon 129 in *PRNP*; M/M = methionine homozygosity at codon 129 in *PRNP*; PrP = prion protein.

Table 2 *Comparison of clinical features between CJD180 and sCJD*

Features	CJD with MM129			CJD with MV129		
	CJD180	sCJD	*p* value	CJD180	sCJD	*p* value
Age at onset, y	70.3 ± 3.9 (n = 4)	65.3 ± 11.6 (n = 116)	0.32	74.8 ± 9.5 (n = 5)	62.6 ± 10.5 (n = 5)	<0.05
Myoclonic jerk, mo*†	8.0 ± 4.5 (n = 4)	2.7 ± 2.4 (n = 113)	<0.01	9.8 ± 3.9 (n = 4)	8.2 ± 5.1 (n = 5)	0.71
Akinetic mutism, mo*‡	11.3 ± 2.2 (n = 4)	3.5 ± 2.8 (n = 113)	<0.005	17.0 ± 1.4 (n = 5)	10.4 ± 5.4 (n = 5)	<0.05
Visual symptom, %§	0.0 (n = 4)	24.0 (n = 96)	0.26	0.0 (n = 5)	20.0 (n = 5)	0.29
Cerebellar symptom, %§	0.0 (n = 4)	12.5 (n = 96)	0.45	0.0 (n = 5)	40.0 (n = 5)	0.11
Higher cortical dysfunction, %§	75.0 (n = 4)	5.2 (n = 96)	<0.0001	60.0 (n = 5)	0.0 (n = 5)	<0.05
NSE value, ng/mL‖	36.7 ± 33.5 (n = 2)	75.9 ± 65.7 (n = 66)		25.9 ± 6.1 (n = 4)	50.6 ± 7.9 (n = 2)	
Positive rate of NSE, %‖¶	50.0 (n = 2)	72.7 (n = 66)		0.0 (n = 4)	100.0 (n = 2)	
Positive rate of 14-3-3 protein, %‖	0.0 (n = 1)	87.7 (n = 65)		66.7 (n = 3)	100.0 (n = 2)	
PSWC in EEG, %	0.0 (n = 4)	94.0 (n = 116)	<0.0001	0.0 (n = 5)	60.0 (n = 5)	<0.05

Values are means ± SD where applicable.

* The duration until the appearance of referring symptoms.
† Patient 1 had not demonstrated myoclonic jerk 15 mo after the onset, and we accepted 15 mo for the statistical comparison. Patient D[5] demonstrated myoclonic jerk, but we could not identify the duration until the appearance. Therefore, we eliminated Patient D from the statistical comparison.
‡ Patients 1 and 4 had not become akinetic and mute, and we could not identify the date when Patient D[5] become akinetic and mute. Therefore, for the statistical comparison, we accepted the date when they were last confirmed not to be akinetic and mute, i.e., 15 mo for Patient 1, 16 mo for Patient 4, and 18 mo for Patient D.
§ The rate of referring symptoms as initial symptoms.
‖ NSE or 14-3-3 protein in CSF.
¶ The cut-off value was 35.0 ng/mL.

CJD = Creutzfeldt–Jakob disease; sCJD = sporadic CJD; NSE = neuron-specific enolase; PSWC = periodic sharp and wave complex.